© 2018. Published by The Company of Biologists Ltd | Journal of Cell Science (2018) 131, jcs209114. doi:10.1242/jcs.209114

RESEARCH ARTICLE

Yeast Hog1 proteins are sequestered in stress granules during high-temperature stress

Kosuke Shiraishi[1], Takahiro Hioki[1], Akari Habata[1], Hiroya Yurimoto[1] and Yasuyoshi Sakai[1,2,*]

ABSTRACT

The yeast high-osmolarity glycerol (HOG) pathway plays a central role in stress responses. It is activated by various stresses, including hyperosmotic stress, oxidative stress, high-temperature stress and exposure to arsenite. Hog1, the crucial MAP kinase of the pathway, localizes to the nucleus in response to high osmotic concentrations, i.e. high osmolarity; but, otherwise, little is known about its intracellular dynamics and regulation. By using the methylotrophic yeast *Candida boidinii*, we found that CbHog1-Venus formed intracellular dot structures after high-temperature stress in a reversible manner. Microscopic observation revealed that CbHog1-mCherry colocalized with CbPab1-Venus, a marker protein of stress granules. Hog1 homologs in *Pichia pastoris* and *Schizosaccharomyces pombe* also exhibited similar dot formation under high-temperature stress, whereas *Saccharomyces cerevisiae* Hog1 (ScHog1)-GFP did not. Analysis of CbHog1-Venus in *C. boidinii* revealed that a β-sheet structure in the N-terminal region was necessary and sufficient for its localization to stress granules. Physiological studies revealed that sequestration of activated Hog1 proteins in stress granules was responsible for downregulation of Hog1 activity under high-temperature stress.

This article has an associated First Person interview with the first author of the paper.

KEY WORDS: Hog1, Yeast, High-temperature stress, Stress granule

INTRODUCTION

Mitogen-activated protein kinases (MAPKs), signaling proteins that are conserved from yeasts to human, are serine-threonine protein kinases activated by extracellular stimuli, such as cytokines, growth factors, hormones and various environmental stresses (Brewster et al., 1993; Herskowitz, 1995; Horvitz and Sternberg, 1991). MAPKs are catalytically inactive in their baseline forms, and phosphorylation of the activation loop is required for activation. When cells sense certain stimuli, small GTPases are activated that trigger downstream signaling pathways, including the MAPK cascade. Dephosphorylation of MAPKs by MAPK phosphatase leads to their inactivation (Cobb and Goldsmith, 1995).

In the baker's yeast *Saccharomyces cerevisiae* (indicated in constructs by the prefix Sc) Hog1 (ScHog1), the ortholog of mammalian MAPK p38 (MAPK14), plays a central role as a signaling mediator during osmoregulation (Brewster and Gustin, 2014). Activated Hog1 is localized to the nucleus and upregulates nearly 600 genes by phosphorylating osmoresponsive transcription factors, such as Msn2 and Msn4, Sko1, Hot1, and Smp1 (Hohmann, 2002), resulting in expression of chaperones and other general stress-response genes (Morano et al., 2012). One major role of the Hog1 pathway is elevation of the intracellular levels of glycerol – which acts as an osmolyte – by inducing glycerol synthesis and accumulation. Loss of Hog1 activity results in abnormal cell morphology (Brewster et al., 1993) and reduced cell growth on high-osmolarity medium. In addition to high osmolarity, Hog1 is partially activated by high-temperature stress through the Sho1 cascade. Inactivation of the Hog1 phosphatases Ptp2 or Ptp3 results in sensitivity to high temperatures (Winkler et al., 2002).

Conditions of high-temperature induce several heat stress-responsive pathways, including the cell wall integrity and Hog1 pathways, together with the formation of two intracellular granule structures, i.e. processing bodies (P-bodies) and stress granules (SGs) (Brengues et al., 2005; Kedersha et al., 2005), which contain non-translating mRNPs (messenger ribonucleoproteins). These granules harbor mRNA decay machinery, and various factors involved in translational impairment and transient storage of mRNAs and, thus, play important roles in quality control of cytosolic mRNAs (Borbolis and Syntichaki, 2015). In addition to these roles, roles of SGs have been recently expanded to include regulation of intracellular signaling pathway by sequestering signaling molecules under stress conditions. For example, signaling through the target of rapamycin complex 1 (TORC1) pathway, which coordinates nutrient availability, was shown to be modulated by sequestration of TORC1 in SGs under conditions of high temperature in *S. cerevisiae* (Takahara and Maeda, 2012). In the fission yeast *Schizosaccharomyces pombe*, calcinurin, the Ca^{2+}/calmodulin-dependent protein phosphatase, localized to SGs in response to heat shock and negatively regulated the assembly of SGs (Higa et al., 2015). As for regulation of the MAPK pathway, RACK1, the scaffold protein binding to MTK1 MAPKKK in mammalian cells, was sequestered in SGs under certain types of stress, such as hypoxia, heat shock and arsenite, to suppress MTK1-mediated signaling pathways (Arimoto et al., 2008).

The methylotrophic yeast *Candida boidinii* survives and proliferates on growing plant leaves, assimilating methanol and nitrate for its survival (Kawaguchi et al., 2011; Shiraishi et al., 2015). Therefore, *C. boidinii* needs to respond and adapt to a wide variety of stresses and environmental changes, including nutrient limitation, high flux of UV radiation, and changes in temperature and osmolarity. In this study, we have investigated the intracellular dynamics of *C. boidinii* (indicated in constructs by the prefix Cb) Hog1 (CbHog1) by using a fusion protein of CbHog1 and the YFP Venus (CbHog1-Venus). Under conditions of high temperature, CbHog1-Venus formed intracellular dot structures that colocalized with the SG marker polyadenylate-binding protein 1 (Pab1) of *C. boidinii* (CbPab1) fused to Venus (CbPab1-Venus). The N-terminal region of CbHog1 was necessary and sufficient for recruitment of CbHog1 to SGs. Further analyses revealed that

[1]Division of Applied Life Sciences, Graduate School of Agriculture, Kyoto University, Kitashirakawa-Oiwake, Sakyo-ku, 606-8502, Kyoto, Japan. [2]Research Unit for Physiological Chemistry, the Center for the Promotion of Interdisciplinary Education and Research, Kyoto University, 606-8502, Kyoto, Japan.

*Author for correspondence (ysakai@kais.kyoto-u.ac.jp)

Y.S., 0000-0002-9831-3085

Received 30 July 2017; Accepted 22 November 2017

Journal of Cell Science (2018) 131, jcs209114. doi:10.1242/jcs.209114

intracellular sequestration of Hog1 under high-temperature conditions is involved in downregulating the activity of phosphorylated Hog1 *in vivo*.

RESULTS

CbHog1 is necessary to tolerate high osmotic stress

We searched the draft genome sequences of *C. boidinii*, and found an 1194-bp open reading frame (ORF) encoding a protein of 398 amino acids (aa), i.e. CbHog1, sharing a high degree of identity with ScHog1 (71%) as well as other yeast Hog1 proteins, *Pichia pastoris* (indicated in constructs by the prefix Pp) Hog1 (PpHog1; 78%) and *Schizosaccharomyces pombe* (indicated in constructs by the prefix Sp) Sty1 (SpSty1; 72%) (Fig. S1A). Based on aa alignment of CbHog1 with ScHog1 (Fig. S1A), we found that CbHog1 contained key conserved aa, including the K50 residue necessary for kinase activity and two phosphorylation sites, T172 and Y174 (Murakami et al., 2008). When compared with Hog1 proteins from other yeast species, ScHog1 had a non-conserved extended region of 37–87 aa at its C-terminus.

The *CbHOG1* gene was disrupted by replacing the ORF with the *CbURA3* gene as a selective marker. In *S. cerevisiae*, Hog1 is localized to the nucleus under hyperosmotic stress, and the *ScHOG1* deletion (*Schog1*Δ) strain exhibits hyper-osmosensitivity (Brewster et al., 1993). We expressed CbHog1-Venus under its own promoter in the *CbHOG1* deletion (*Cbhog1*Δ) strain. CbHog1-Venus was localized to the nucleus 5 min after a shift to medium containing 0.5 M NaCl (Fig. S1B). Stress resistance analysis was also performed under conditions of high osmolarity in wild type, *Cbhog1*Δ, and CbHog1-Venus expressing *Cbhog1*Δ strains. The *Cbhog1*Δ strain exhibited severe growth defects on YPD medium containing 0.5 M NaCl, and CbHog1-Venus completely complemented the growth defect of the *Cbhog1*Δ strain under 0.5 M NaCl (Fig. S1C). These results indicate that, similar to ScHog1, CbHog1 functions in osmotic stress tolerance in *C. boidinii*.

CbHog1-Venus forms intracellular dot structures under high-temperature condition

To examine the intracellular dynamics of CbHog1-Venus under high-temperature stress, *C. boidinii* cells expressing CbHog1-Venus were incubated at different temperatures (34–45°C) for 30 min, and then observed under a fluorescent microscope. *C. boidinii* was unable to proliferate at temperatures above 35.5°C (Fig. S2A), and *C. boidinii* cells incubated at high temperatures contained intracellular dot structures of CbHog1-Venus in the cytosol (Fig. 1A). Morphometric analysis revealed a positive correlation between the incubation temperature and the number of CbHog1-Venus dots from 35.5–42°C (Fig. 1B).

Nuclear localization of CbHog1-Venus under high-temperature condition was examined with cell samples incubated at 42°C for 30 min. Cells stained with DAPI were microscopically observed and showed that significant localization of CbHog1-Venus to the nucleus was not observed in *C. boidinii* at 42°C, whereas a few dots of CbHog1-Venus were associated with the blue fluorescence of DAPI (Fig. S3A). This indicated that nuclear localization of CbHog1 was not a major event in *C. boidinii* under high-temperature conditions.

Interestingly, we observed that PpHog1 fused to YFP (PpHog1-YFP) in *P. pastoris* and SpSty1-GFP in *S. pombe* formed similar dots under high-temperature stress, whereas ScHog1 fused to GFP (ScHog1-GFP) in *S. cerevisiae* did not (Fig. 1C).

To examine whether this dot formation was due to irreversible aggregation of the protein, we monitored CbHog1-Venus fluorescence after reducing the high temperature (42°C) again. As

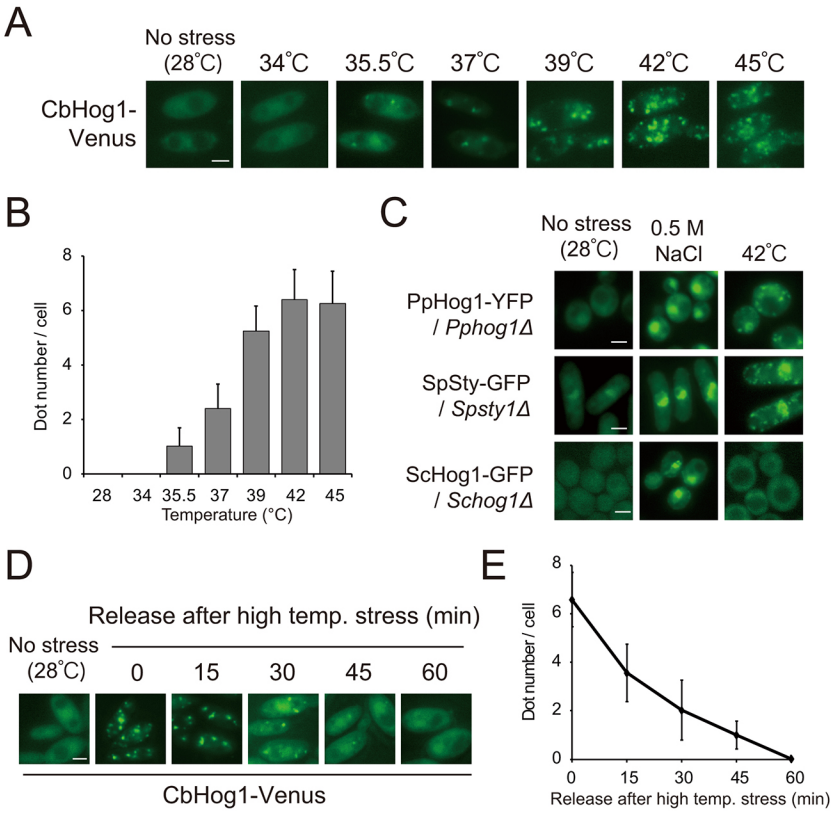

Fig. 1. Intracellular localization of CbHog1 under conditions of high temperature. (A) Microscopic images of the *Cbhog1*Δ strain expressing CbHog1-Venus under conditions of normal and high temperature. (B) Quantification of the number of Venus dots per cell in the *Cbhog1*Δ strain expressing CbHog1-Venus; the same strain was used for the microscopic imaging analysis shown in A. (C) Intracellular dot structures of three yeast species (*P. pastoris*, *S. cerevisiae*, *S. pombe*) expressing fluorescence-tagged Hog1 fusion proteins under high-salt or high-temperature stress. The *Pphog1*Δ strain expressing PpHog1-YFP, the *Spsty1*Δ strain expressing SpSty1-GFP, and the *Schog1*Δ strain expressing ScHog1-GFP were analyzed by fluorescence microscopy. Cells were grown to early log phase and then subjected to high-salt stress (0.5 M NaCl, 5 min), or high-temperature stress (42°C, 30 min). (D) Microscopic images of the *Cbhog1*Δ strain expressing CbHog1-Venus after removal of high-temperature stress. Cells grown to early log phase in SD medium at 28°C were subjected to high-temperature stress (39°C, 30 min), and then the intracellular dynamics of CbHog1-Venus was observed by fluorescence microscopy during recovery at 28°C for 60 min. (E) Quantification of the number of Venus dots per cell in the *Cbhog1*Δ strain expressing CbHog1-Venus; the same strain was used for the microscopic imaging analysis shown in D. Each sample contained a minimum of 50 cells. Error bars show ±s.d. of all cells. Scale bars: 2 µm.

Journal of Cell Science (2018) 131, jcs209114. doi:10.1242/jcs.209114

shown in Fig. 1D and E, CbHog1-Venus dots gradually disappeared after the shift from 42°C to 28°C, and very few cells harbored CbHog1-Venus dots 60 min after release from heat. These findings indicated that dot formation of CbHog1-Venus is a reversible process, rather than a consequence of irreversible aggregation of the protein.

High-temperature stress induces sequestration of CbHog1 into SGs

SGs are cytosolic complexes composed of proteins and RNAs that appear in response to external stresses, such as heat shock and severe ethanol stresses (Buchan et al., 2011; Kato et al., 2011).

First, we cloned the DNAs coding for SG marker proteins in *C. boidinii*. A search of the *C. boidinii* draft genome sequence revealed putative SG proteins, including the poly-A-binding protein Pab1 and the Pab1-binding protein Pbp1 (Table S1). As in *S. cerevisiae*, high-temperature condition induced formation of cytosolic dots of both CbPab1-Venus and CbPbp1 fused to mCherry (CbPbp1-mCherry), and dots corresponding to these two SG proteins were colocalized in the cytosol (Fig. 2A). When *C. boidinii* cells expressing CbHog1-mCherry and CbPab1-Venus were shifted to 42°C, both CbHog1-mCherry and CbPab1-Venus formed dot structures, and most CbPab1-Venus dots colocalized with CbHog1-mCherry (Fig. 2B,C). These results indicate that, after shift to high temperature, SG formation is induced and CbHog1 is recruited to SGs.

SpSty1 was reported to affect formation of SGs under stress conditions of high osmolarity in *S. pombe* (Nilsson and Sunnerhagen, 2011). In the *SpSTY1* deletion (*Spsty1*Δ) strain, the appearance of *S. pombe* poly-A-binding protein (SpPabp) fused to red fluorescent protein (SpPabp-RFP) as dots was markedly delayed during high-osmolarity stress but not under glucose deprivation condition. We investigated whether CbHog1 affected formation of SGs under high-temperature stress in *C. boidinii*. When the *Cbhog1*Δ strain expressing CbPab1-Venus was shifted to 42°C, CbPab1-Venus formed dots (Fig. 2D) as observed in the wild-type background (Fig. 2A). Therefore, the effect of CbHog1 was limited, if any, on the formation of SGs after shift to high temperature.

Next, to determine whether the activated form of CbHog1 is necessary for recruitment to SGs, we tested mCherry- or Venus-tagged CbHog1(K50R), a kinase-dead mutant lacking the phosphotransfer domain necessary for activity, for its recruitment to SGs. This mutation, indeed, decreased survival of *C. boidinii* in medium containing 0.5 M NaCl (Fig. S2B), suggesting loss of CbHog1 activity. Cytosolic dot structures of CbHog1(K50R)-Venus were observed under high-temperature stress (Fig. 2E,F), and

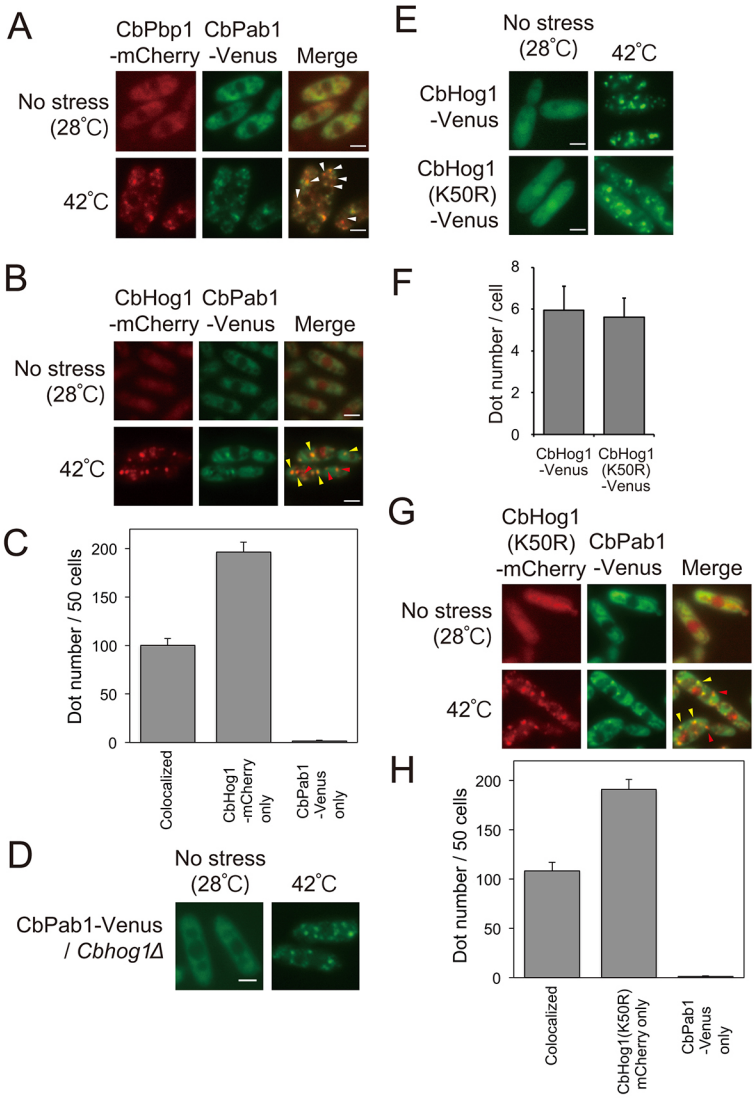

Fig. 2. CbHog1 is localized to SGs under high-temperature stress. (A) Microscopic images of the *C. boidinii* strain expressing two SG marker proteins, CbPbp1-mCherry and CbPab1-Venus. Cells were grown to early log phase, and then subjected to high-temperature stress at 42°C for 30 min. Merged images were generated by combining the mCherry and Venus fluorescence images. Arrowheads indicate representative dots in which CbPbp1-mCherry colocalized with CbPab1-Venus. (B) Microscopic images of the *C. boidinii* strain expressing CbHog1-mCherry and CbPab1-Venus. Cells were grown to early log phase, and then subjected to indicated high-temperature stress for 30 min. Merged images were generated by combining the mCherry (red) and Venus (green) fluorescence images. Arrowheads indicate representative dots in which CbHog1-mCherry colocalized with CbPab1-Venus. (C) Intracellular localization of CbHog1-mCherry and CbPab1-Venus derived from quantification of 50 cells after high temperature stress for 30 min. Errors bars represent +s.d. of the triplicate measurements. (D) Microscopic images of the *Cbhog1*Δstrain expressing CbPab1-Venus. Cells were grown to early log phase, and subjected to indicated high-temperature stress for 30 min. (E) Microscopic images of the *Cbhog1*Δ strain expressing CbHog1 (K50R)-Venus. Cells were grown to early log phase, and then subjected to high-temperature stress at 42°C for 30 min. (F) Quantification of the number of Venus dots per cell in the *Cbhog1*Δ strain expressing CbHog1(K50R)-Venus; the same strain was used for the microscopic imaging analysis shown in E. Each sample contained a minimum of 50 cells. Error bars show +s.d. of all cells. (G) Microscopic images of the *C. boidinii* strain expressing CbHog1(K50R)-mCherry and CbPab1-Venus. Cells were grown to early log phase, and subjected to high-temperature stress at 42°C for 30 min. Merged images were generated by combining the mCherry and Venus fluorescence images. Arrowheads indicate representative dots in which CbHog1(K50R)-mCherry colocalized with CbPab1-Venus. (H) Intracellular localization of CbHog1(K50R)-mCherry and CbPab1-Venus derived from quantification of 50 cells after high temperature stress for 30 min. Error bars represent +s.d. of the triplicate measurements. Scale bars: 2 µm.

Journal of Cell Science (2018) 131, jcs209114. doi:10.1242/jcs.209114

CbHog1(K50R)-mCherry colocalized with CbPab1-Venus, a SG marker protein (Fig. 2G,H). Therefore, recruitment of CbHog1 to SGs was independent of CbHog1 activity.

Next, we investigated whether CbHog1-mCherry dots colocalized with P-bodies, another type of RNP granule. However, only 10% of dots indicating the presence of the P-body marker protein CbEdc3-Venus were associated with CbHog1-mCherry dots (Fig. S3B and Table S2).

Interestingly, CbHog1-mCherry formed dot structures not only in *C. boidinii,* but also in *S. cerevisiae* under high-temperature stress (Fig. S3C), whereas ScHog1-Venus did not form dot structures in *S. cerevisiae* (Fig. 1C). Therefore, we speculate that recruitment of CbHog1-mCherry to SGs is due to its aa sequence.

A β-sheet structure at the N-terminal region of CbHog1 is important for its recruitment to SGs

CbHog1 contains three conserved sequences, the common docking (CD) site (aa 300–314), the PBD-2 binding domain (PBD-2; aa 318–348), and the kinase domain (KD; aa 21–299) including the putative phosphotransfer domain (PPD; aa 47–52) and two phosphorylation sites (T174 and Y176) (Murakami et al., 2008) (Fig. 3A). We wanted to determine which regions on CbHog1 were necessary and sufficient for its recruitment to SGs.

Wild-type CbHog1-Venus formed around six fluorescent dots per cell (Fig. 3B,C). We constructed various truncated variants, and observed dot formation after shift to high temperature. The N-terminal deletion analysis (Fig. 3B) revealed that removal of the N-terminal region (aa 1–41) of CbHog1 drastically decreased dot formation. However, deletion of neither the KD domain nor the PBD-2 domain in the C-terminal region decreased CbHog1-Venus dot numbers (Fig. 3B,C). Further deletion analyses revealed that the N-terminal 30-aa sequence of CbHog1 was sufficient for partial localization, and the N-terminal 50-aa sequence of CbHog1 was sufficient for full recruitment of CbHog1-GFP to SGs (Fig. 3C).

Prediction of protein structure based on homology modeling revealed that the N-terminal region of CbHog1 is likely to assume a β-sheet structure with high hydrophobicity (Fig. 4A). CbHog1Δ(1-20)-Venus was partially localized to SGs, whereas CbHog1Δ(1-41)-

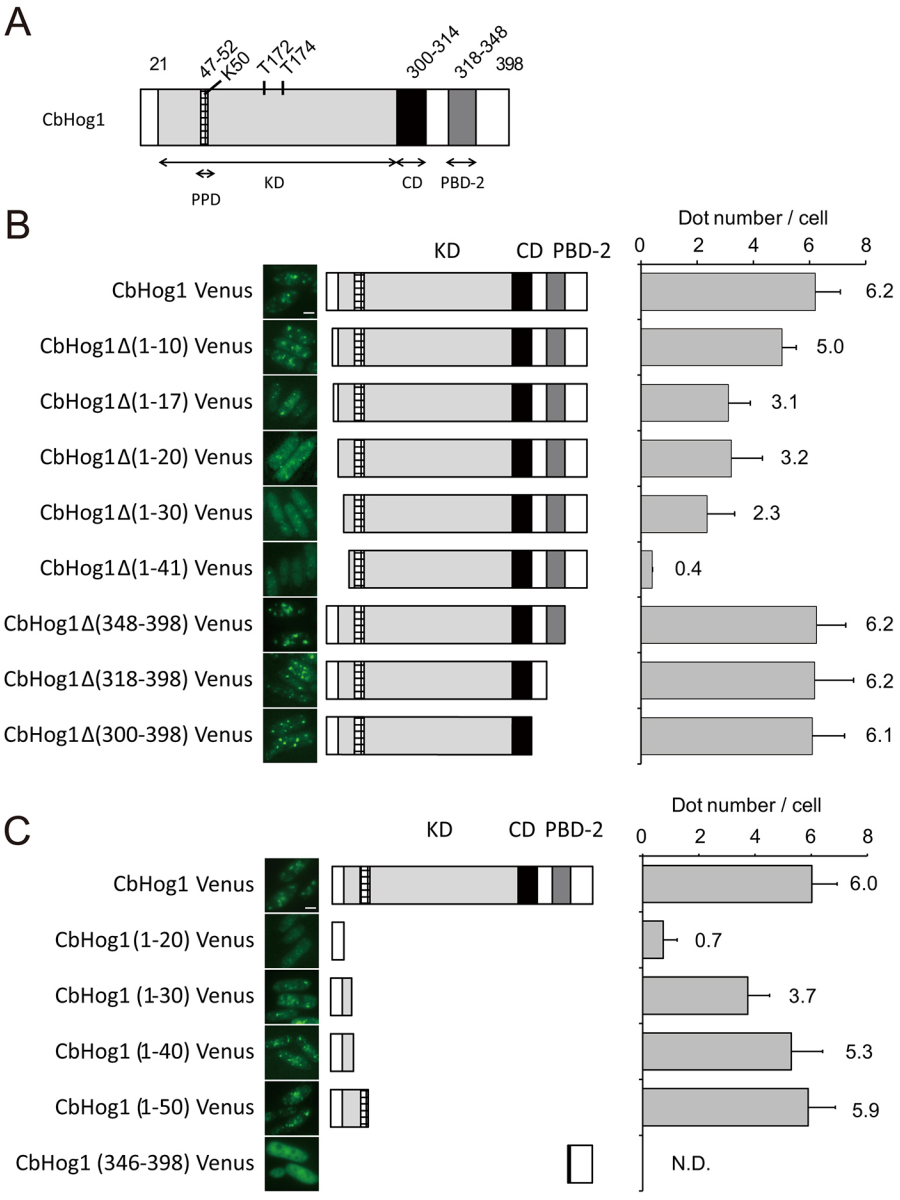

Fig. 3. The N-terminal region of CbHog1 is necessary and sufficient for dot formation. (A) Schematic diagram of the CbHog1. PPD, putative phosphorylation domain; KD, kinetic domain; CD, catalytic domain; PBD-2, Pbs2-binding domain 2; K50, conserved lysine residue; T172, conserved threonine residue; Y174, conserved tyrosine residue. (B) Microscopic images and numbers of Venus dots per cell in *Cbhog1*Δ strains expressing CbHog1Δ(1-10)-Venus, CbHog1Δ(1-17)-Venus, CbHog1Δ(1-20)-Venus, CbHog1Δ(1-30)-Venus, CbHog1Δ(1-41)-Venus, CbHog1Δ(348-398)-Venus, CbHog1Δ(318-398)-Venus, or CbHog1Δ(300-398)-Venus. Cells were grown to early log phase in SD medium, and then subjected to high-temperature stress (42°C, 30 min). (C) Microscopic images and the numbers of Venus dots per cell in *C. boidinii hog1*Δ strains expressing CbHog1(1-20)-Venus, CbHog1Δ(1-30)-Venus, CbHog1Δ(1-40)-Venus, CbHog1(1-50)-Venus, or CbHog1(346-398)-Venus. Cells were grown to early log phase in SD medium, and then subjected to high-temperature stress (42°C, 30 min). N.D., not determined. Error bars show +s.d.

Journal of Cell Science (2018) 131, jcs209114. doi:10.1242/jcs.209114

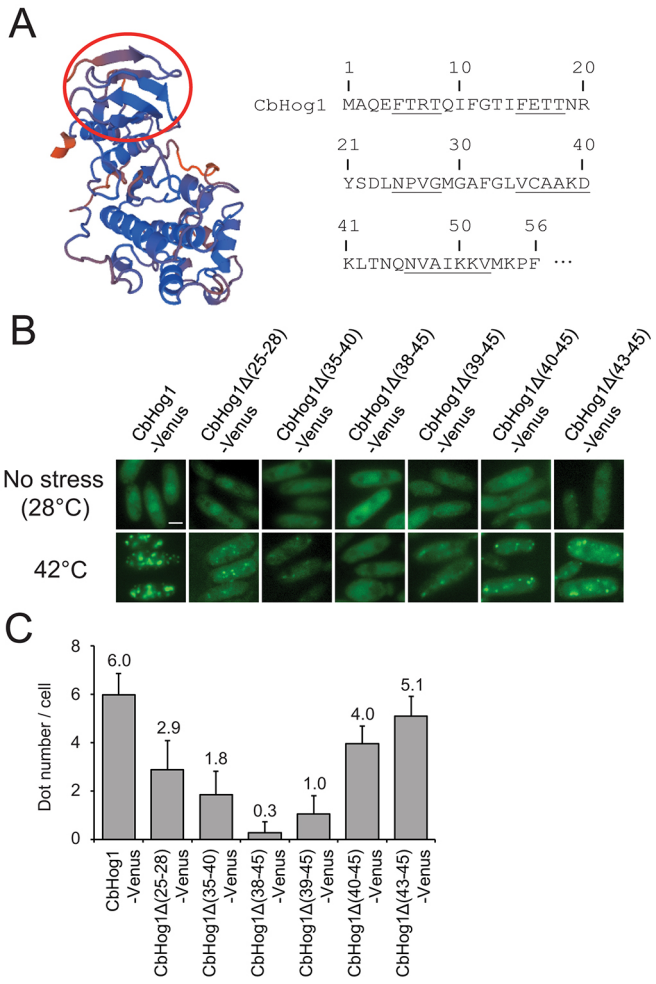

Fig. 4. A β-sheet structure in the N-terminal region of CbHog1 contributes to dot formation. (A) Left panel, predicted structure of CbHog1 based on homology modeling (SWISS-MODEL: http://swissmodel.expasy.org/). The β-sheet structure in the N-terminal region (~50 aa residues) is encircled by a red line. Right panel, each underlined aa residue is predicted to constitute one of the β-sheet strands. (B) Microscopic images of *Cbhog1*Δ strains expressing CbHog1Δ(25-28)-Venus, CbHog1Δ(35-40)-Venus, CbHog1Δ(38-45)-Venus, CbHog1Δ(39-45)-Venus, CbHog1Δ(40-45)-Venus, or CbHog1Δ(43-45)-Venus. Cells were grown to early log phase in SD medium, and then subjected to high-temperature stress (42°C, 30 min). (C) Quantification of the number of Venus dots per cell in the *Cbhog1*Δ strain expressing CbHog1-Venus; the same strain was used for the microscopic imaging analysis shown in B. Each sample contained a minimum of 50 cells. Error bars show +s.d. of all cells. Scale bar: 2 µm.

Venus was not recruited to SGs (Fig. 3B). Therefore, we speculated that the second β-sheet structure composed of aa ^{25}NPVG^{28} and ^{35}VCAAKD^{40} has a greater contribution to SG localization than the first β-sheet structure composed of aa ^{5}FTRT^{8} and ^{15}FETT^{18}. More-detailed deletion analyses revealed that CbHog1Δ(38-45)-Venus did not exhibit SG localization but, instead, dispersed in the cytosol (Fig. 4B,C). CbHog1Δ(35-40)-Venus and CbHog1Δ(39-45)-Venus were also defective in recruitment to SGs (Fig. 4B,C). Homology remodeling predicted that the 38-45 aa deletion of CbHog1 disrupted the second β-sheet structure (Fig. 4A). Taken together, these observations show that the β-sheet structures in the N-terminus region of CbHog1 (20-41) plays a critical role in recruitment of CbHog1 to SGs under high-temperature stress.

Removal of non-conserved C-terminal region of ScHog1 enabled dot formation under high-temperature stress

As shown above, and in contrast to other yeast Hog1-family proteins, ScHog1-Venus did not form dot structures under high-temperature stress in *S. cerevisiae* (Fig. 1C). Likewise, in *C. boidinii*, ScHog1-Venus was not recruited to SGs under high-temperature stress (Fig. 5A). Alignment of the aa sequences of Hog1 homologs (Fig. S1A) revealed that ScHog1 harbors a long C-terminal region that is not conserved in the other three yeast species. Based on the predicted structure (Fig. 4A), we speculated that this C-terminal region interferes with the β-sheet structure in the N-terminal region that is involved in the recruitment of ScHog1-Venus to SGs. To test this idea, we introduced ScHog1(1-350)-Venus lacking the C-terminal 85 aa residues into the *Cbhog1*Δ strain. Under high-temperature stress, ScHog1(1-350)-Venus was recruited to SGs not only in *S. cerevisiae*, but also in *C. boidinii* (Fig. 5B). However, CbHog1-ScHog1(351-435)-Venus formed dots under high-temperature stress in *C. boidinii* (Fig. S3D), indicating that the non-conserved C-terminal region of ScHog1 is necessary but not sufficient to prevent dot formation of ScHog1 in *C. boidinii*.

Active Hog1 protein dispersed in the cytosol induces cell death under high-temperature stress

What is the physiological role of recruitment of CbHog1 to SGs under high-temperature stress? To answer this question, we first focused on the phosphorylation of CbHog1-Venus. As shown in Fig. S4, a band shift to a higher molecular mass was observed on Phos-tag-SDS-PAGE in cells exposed to high-temperature stress for 15 min, and also in cells exposed to 0.5 M NaCl. These results indicated that CbHog1 is phosphorylated and exists in the activated form under high-temperature stress. Because the N-terminal region of CbHog1 critical for recruitment to SGs is close to K50 – a critical aa residue for Hog1 activity in the KD domain – we sought to identify a mutant that lost the ability to be recruited to SGs but retained Hog1 kinase activity. Among the mutants impaired in recruitment to SGs (Fig. 3B,C, and Fig. 4C) – with Cb-Hog1Δ (38–45)-Venus and CbHog1Δ(35–40)-Venus not supporting

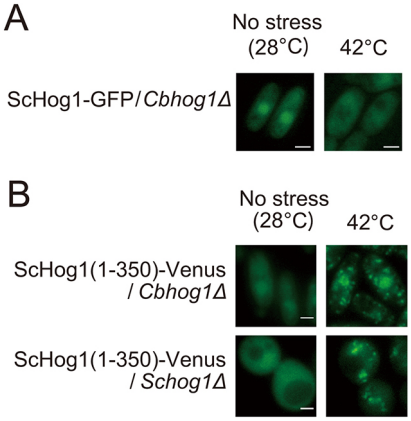

Fig. 5. Intracellular localization of ScHog1 in *C. boidinii* and *S. cerevisiae* under high-temperature stress. (A) Microscopic images of the *Cbhog1*Δ strain expressing ScHog1-Venus under the control of the *CbACT1* promoter. Cells were grown to early log phase in SD medium, and then subjected to high-temperature stress (42°C, 30 min). (B) Microscopic images of the *Cbhog1*Δ strain or the *Schog1*Δ strain expressing ScHog1(1-350). Cells were grown to early log phase in SD medium, and then subjected to high-temperature stress (42°C, 30 min). Scale bars: 2 µm.

Journal of Cell Science (2018) 131, jcs209114. doi:10.1242/jcs.209114

growth in the presence of 0.5 M NaCl – the CbHog1Δ(1–17)-Venus mutant fully complemented and CbHog1Δ(25–28)-Venus partially complemented the growth of *Cbhog1*Δ in medium containing 0.5 M NaCl (Fig. 6). Therefore, CbHog1Δ(1–17)-Venus and CbHog1Δ (25–28)-Venus were identified as mutants that retained Hog1 activity while their efficiency of recruitment to SGs was reduced to ∼50% (Figs 3B and 4C).

Next, we spotted serially diluted cell suspensions onto YPD plates and incubated at 37°C for 24 h, cellular survival under high-temperature stress (after growth at 28°C) was then assessed. Although CbHog1-Venus (wild type), CbHog1Δ(38-45)-Venus (inactive Hog1), CbHog1Δ(35-40)-Venus (inactive Hog1) and *Cbhog1*Δ exhibited comparable levels of cellular survival under high-temperature stress (Fig. 6), survival was diminished in CbHog1Δ(1-17)-Venus and CbHog1Δ(25-28)-Venus (active but impaired in recruitment to SGs) (Fig. 6A-C). We also examined the cellular survival in cells expressing CbHog1Δ(1-10)-Venus, which fully complemented the growth of the *Cbhog1*Δ strain in medium containing 0.5 M NaCl (Fig. 6C). No growth defect was detected with CbHog1Δ(1-10)-Venus. These results showed that cytosolic and active CbHog1 inhibited the growth of *C. boidinii* and decreased cellular survival under high-temperature stress, suggesting that recruitment of active CbHog1 to SGs impedes Hog1-induced cell death under high-temperature stress.

We also examined ScHog1-Venus protein and its variants in *C. boidinii.* Similar to CbHog1-Venus, ScHog1-Venus was transported to the nucleus and complemented the growth defect of *Cbhog1*Δ in the presence of 0.5 M NaCl (Fig. 7A,B). Thus, ScHog1-Venus was confirmed to be active and functional in *C. boidinii*. Under conditions of high temperature, ScHog1-Venus dispersed into the cytosol in *C. boidinii* (Fig. 7A), and *C. boidinii* cells expressing ScHog1-Venus lost cell viability under high-temperature stress (Fig. 7B). Therefore, we used well-characterized ScHog1 and mutant proteins to study the relationship between Hog1 activity and the decrease in cellular survival in response to high-temperature stress in *C. boidinii*.

ScHog1 is phosphorylated on aa residues T174 and Y176 by the MAPKK Pbs2 (Brewster et al., 1993). Activation of ScHog1 leads to its Nmd5p-dependent nuclear import (Ferrigno et al., 1998), and it subsequently functions as a kinase through its PPD containing K52 (Hall et al., 1996). Neither the *Cbhog1*Δ strain expressing ScHog1(K52R)-Venus (KD mutant) nor the *Cbhog1*Δ strain expressing ScHog1(T174A/Y176F)-Venus (the phosphorylation defective mutant) was able to grow under 0.5 M NaCl (Fig. 7B), although ScHog1(K52R)-Venus and ScHog1(T174A/Y176F)-Venus translocated into the nucleus in *C. boidinii* (Fig. 7A). Under conditions of high temperature, they dispersed in the cytosol in *C. boidinii* (Fig. 7A), and cells expressing these inactive Hog1 variants exhibited the same cellular survival level as the wild-type strain under high-temperature stress (Fig. 7B). These results confirmed that active ScHog1-Venus dispersed in the cytosol induced cell death under high-temperature stress.

Active ScHog1 sequestered in SGs or artificially anchored to the plasma membrane suppresses the cytotoxicity of ScHog1 under high-temperature stress

Finally, we studied whether intracellular sequestration of active ScHog1 affects its cytotoxicity. As shown above, ScHog1(1-350)-Venus was recruited to SGs after a shift to high temperature in *C. boidinii* (Fig. 5B). ScHog1(1-350)-Venus was able to complement the growth defect of the *Cbhog1*Δ strain under 0.5 M NaCl, confirming that the protein was functional. As shown in Fig. 7C,

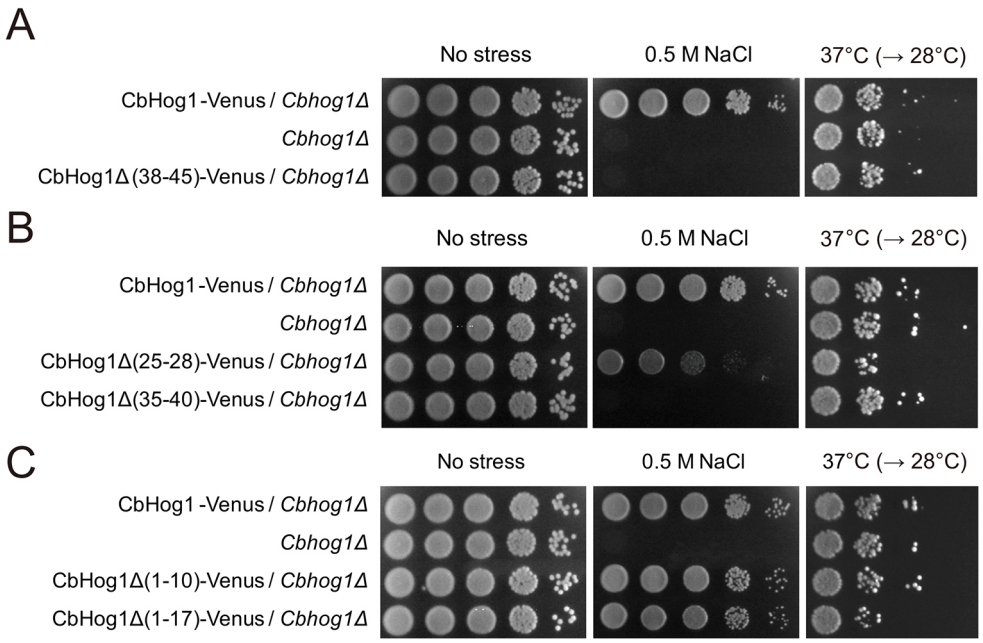

Fig. 6. Dot formation by CbHog1 under high-temperature stress is important for cell survival. Growth assay of cells grown under conditions of high-salt or high-temperature stress. Cells were grown to early log phase, adjusted to OD_{610}=1, and 3 µl of tenfold serial dilutions were dropped onto YPD plates with or without 0.5 M NaCl. Subsequently, one plate containing 0.5 M NaCl and one without additional NaCl were incubated at 28°C, and one plate without additional NaCl was treated subjected to temperature stress (37°C, 24 h) before incubation at 28°C. Cell growth was scored after 2 days. (A) Growth of the *Cbhog1*Δ strain expressing CbHog1Δ(38-45)-Venus was compared to that of the *Cbhog1*Δ strain expressing CbHog1-Venus and *Cbhog1*Δ strain. (B) Growth of the *Cbhog1*Δ strain expressing CbHog1Δ(25-28)-Venus or CbHog1Δ(35-40)-Venus was compared to that of the *Cbhog1*Δ strain expressing CbHog1-Venus and *Cbhog1*Δ strain. (C) Growth of the *Cbhog1*Δ strain expressing CbHog1Δ(1-10)-Venus or CbHog1Δ(1-17)-Venus was compared to that of the *Cbhog1*Δ strain expressing CbHog1-Venus and the *Cbhog1*Δ strain alone.

Journal of Cell Science (2018) 131, jcs209114. doi:10.1242/jcs.209114

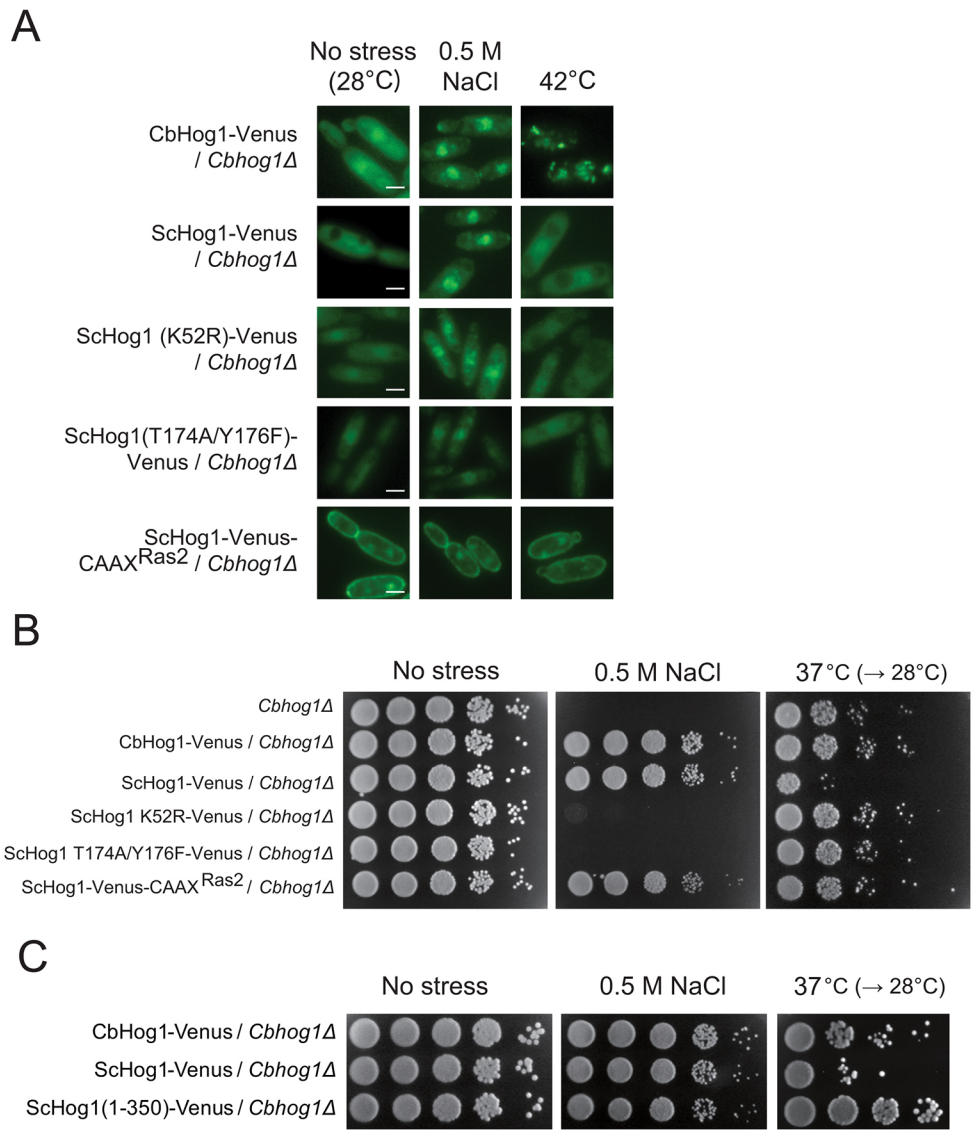

Fig. 7. Intracellular sequestration of Hog1 suppresses cytotoxicity of ScHog1 under high-temperature stress in *C. boidinii*. (A) Microscopic images of the *Cbhog1*Δ strains expressing CbHog1-Venus, ScHog1-Venus, ScHog1(K52R)-Venus, ScHog1(T174A/Y176F)-Venus, and ScHog1-Venus-CAAX^{Ras2}. Cells were grown to early log phase in SD medium, and subjected to stress of high temperature (42°C, 30 min) or high osmolarity. (B) Growth assay of cells cultured under high-salt or high-temperature conditions. Cells were grown to early log phase, adjusted to OD_{610}=1, and 3 µl of tenfold serial dilutions were dropped onto YPD plates with or without 0.5 M NaCl. Subsequently, one plate containing 0.5 M NaCl and one without additional NaCl were incubated at 28°C, and one plate without additional NaCl was subjected to high-temperature stress (37°C, 24 h) before incubation at 28°C. Cell growth was scored after 2 days. Growth of *Cbhog1*Δ strains expressing ScHog1-Venus, ScHog1 (K52R)-Venus, ScHog1(T174A/Y176F)-Venus, or ScHogg1-Venus-CAAX^{Ras2} was compared to that of the *Cbhog1*Δ strain expressing CbHog1-Venus and the *Cbhog1*Δ strain alone. (C) Growth of the *Cbhog1*Δ strain expressing ScHog1(1-350) was compared to that of the *Cbhog1*Δ strain expressing CbHog1-Venus and the *Cbhog1*Δ strain alone. Growth conditions were the same as in B. Scale bars: 2 µm.

deletion of 85 aa from the C-terminal region [ScHog1(1-350)-Venus] was able to reduce the cytotoxicity of ScHog1-Venus under high-temperature stress. Accordingly, we speculated that sequestration of ScHog1(1-350)-Venus to SGs impeded cytotoxicity.

Plasma membrane targeting of Ras proteins requires posttranslational modification of the C-terminal CAAX box – in which C=cysteine, A any aliphatic aa and X=any aa – and either palmitoylation or the presence of a polybasic domain (Casey et al., 1989; Deschenes et al., 1989; Hancock et al., 1990). To investigate whether anchoring of active ScHog1-Venus to the plasma membrane can suppress cytotoxicity under high-temperature stress, ScHog1-Venus-CAAX^{Ras2} was expressed in *Cbhog1*Δ cells. ScHog1-Venus-CAAX^{Ras2} was anchored to the plasma membrane (Fig. 7A). In addition, as shown in Fig. 7B, ScHog1-Venus-CAAX^{Ras2} complements the growth defect of *Cbhog1*Δ strain under 0.5 M NaCl and also suppress the cytotoxicity of active ScHog1-Venus under high-temperature stress (Fig. 7B). Therefore, the intracellular sequestration of ScHog1-Venus not only to SGs but also the plasma membrane may impede the function of ScHog1, suggesting that sequestration of yeast Hog1 plays an important role in downregulating yeast Hog1 activity.

DISCUSSION

Recent work has shown that TORC1 is recruited to lysosomal membranes to activate starvation signaling, whereas recruitment to SGs downregulates TORC1 activity (Demetriades et al., 2014; Takahara and Maeda, 2012). Intracellular sequestration of several signaling molecules in SGs has been investigated in relation to their functions (Arimoto et al., 2008; Kim et al., 2005). However, the molecular basis of the recruitment of these signaling factors to SGs and the physiological role of sequestration of these proteins to SGs remain to be elucidated in detail. Here, we revealed that important MAP kinases, the Hog1 proteins, exhibit drastic changes in intracellular localization to SGs under high-temperature stress in different yeast species.

We found that recruitment of CbHog1 to SGs depended on a hydrophobic β-sheet structure on its N-terminal 50 aa, and this is region necessary and sufficient for recruitment to SGs. In other words, recruitment of Hog1 to SGs depends on its own aa sequence. Aa sequences responsible for localization to SGs were analyzed in several proteins that did not affect formation of SGs as with CbHog1 (Bentmann et al., 2012; Weissbach and Scadden, 2012); however, no consensus sequences were determined. CbHog1 was phosphorylated and activated under high-temperature stress.

Because the inactivated form of Hog1 protein was recruited to SGs, activation of Hog1 itself is not required for its recruitment.

Another interesting finding was that removal of the non-conserved C-terminal region of ScHog1 enabled recruitment of ScHog1 to SGs (Fig. 5B) in *S. cerevisiae*. This shows an inherent potential of ScHog1 to be recruited to SGs, which might be negatively regulated by its C-terminal region. Although this C-terminal region of ScHog1 (351-435) is necessary to prevent dot formation of ScHog1 proteins in *C. boidinii* and *S. cerevisiae* under high-temperature, contrary to our presupposition, CbHog1-ScHog1(351-435)-Venus formed dots in *C. boidinii* (Fig. S3D). We speculate that there is some regulatory mechanism that involves interaction between ScHog1(1-350) and ScHog1(351-435) regions to prevent and regulate dot formation of ScHog1. A database search revealed that Hog1 proteins from *Zygosaccharomyces rouxii*, *Torulaspora delbrueckii*, and *Candida glabrata* also possess C-terminal non-conserved regions similar to that in ScHog1. Although we did not observe recruitment of Hog1 to SGs in these yeasts, regulation of Hog1 recruitment to SGs in *S. cerevisiae*, as well as in the three species mentioned above, remains an open question that awaits further study.

More than 20 proteins were identified as components of yeast SG, and they seem to have some interactions with P-bodies (Buchan and Parker, 2009; Buchan et al., 2011). It should be noted that, although most CbPab1-Venus dots colocalized with CbHog1-mCherry dots, two-thirds of CbHog1-mCherry dots did not show colocalization with CbPab1-Venus dots (Fig. 2B,C,G,H). Two explanations are possible for this observation. First, CbPab1-Venus does not equally represent the total SG population. So colocalizaton of CbPab1-Venus and CbHog1-mCherry inevitably shows only a part of the total colocalization of CbHog1-mCherry and SG. Second, there is a high possibility that CbHog1-mCherry associates with the P-body. Indeed, we observed that about 10% of CbHog1-mCherry dots associated with the P-body marker CbEdc3-Venus (Fig. S3B). As is the case, the dynamic feature of SGs is still to be further explored.

We then investigated the physiological significance of Hog1 sequestration in SGs by using different mutants of CbHog1-Venus and ScHog1-Venus proteins. Initially, we screened for a CbHog1 mutant protein that lacked the ability to be recruited to SGs (as determined by fluorescence microscopy) but retained kinase activity (as determined by the ability to grow in 0.5 M NaCl). Among various strains tested, Cb-Hog1Δ1-17 and Cb-Hog1Δ25-28 exhibited such a phenotype (Fig. 6). Our results with these mutants indicated that the active form of CbHog1 exerted a cytotoxic effect, and that impairment of recruitment to SGs promoted cell death. A previous study reported a negative effect of hyperactivated Hog1 kinase in the absence of two protein phosphatases, Ptp2 and Ptp3, during cell growth at high temperature (Winkler et al., 2002).

To further investigate the effect of Hog1 activity and SG recruitment on cell death, we expressed non-functional ScHog1-Venus mutants (kinase-dead and phosphorylation-defective) in *C. boidinii*. On the one hand, the wild-type ScHog1 protein completely complemented the growth of the *Cbhog1*Δ strain in medium containing 0.5 M NaCl, and previously characterized inactive ScHog1 mutations lost the ability to grow in the presence of high salt concentration (Fig. 7). On the other hand, under high-temperature stress, the wild-type ScHog1 protein dispersed in the cytosol and induced cell death after high-temperature shift, and this activity depended on Hog1 activity. Therefore, ScHog1 protein that was activated under high-temperature stress induces cell death when present in the cytosol. Although ScHog1(1-350) was active and able to complement the growth of *Cbhog1*Δ strain in 0.5 M NaCl, this mutant exhibited less cytotoxicity under high-temperature stress than wild-type ScHog1. These results all suggest that active Hog1 is sequestered to SGs for its downregulation.

The site of intracellular sequestration of Hog1 for downregulation is not necessarily limited to SGs. When ScHog1 was anchored to the plasma membrane (ScHog1-Venus-CAAX^{Ras2}), cytotoxicity under high-temperature stress was reduced, as observed for ScHog1(1-350) (Fig. 7). Therefore, the positive effect of activated Hog1 at SGs is likely to be small. Instead, we speculate that sequestration of cytosolic Hog1 to SGs is a strategy for modulation of Hog1 activity under high-temperature stress.

However, some part within active Hog1 proteins may also be translocated to the nucleus for gene activation. SpSty1-GFP formed cytosolic dots but, simultaneously, localized to the nucleus under high-temperature stress (Fig. 1C). These features indicate that SpSty1 upregulates gene expression in the nucleus to help the cell adapt to high-temperature stress but, at the same time, activity of a fraction of SpSty1 is suppressed by sequestration into dot structures. Compared with other yeast species, SpSty1 might play a more significant and active role in adaptation to high temperature. Consistent with this idea, previous studies have demonstrated that ScHog1 is only important for rapid recovery from high-temperature stress (Winkler et al., 2002), and that the *Spsty1*Δ strain loses the ability to grow at high temperatures (Millar et al., 1995).

In summary, yeast Hog1 is sequestered in SGs under high-temperature condition through its N-terminal hydrophobic β-sheet structure; and we propose that activated Hog1 in the cytosol can be downregulated by this sequestration. As for *S. cerevisiae*, the experimental strain is a conventional baker's yeast that has been preserved in artificial environments for more than 1000 years. By contrast, *C. boidinii*, which proliferates on plant leaves, must adapt to severe environmental changes under natural conditions. Therefore, recruitment of Hog1 to SGs for downregulation might confer a survival advantage in this species. Our results reveal the importance of intracellular sequestration of active Hog1 kinase into SGs, and we believe that elucidation of the underlying molecular mechanisms will – at molecular level – advance our understanding of the physiological role of SGs and the intricate regulation of intracellular signaling pathways.

MATERIALS AND METHODS

Yeast strains and culture conditions

Escherichia coli DH10B was used for plasmid propagation. *E. coli* was grown at 37°C in lysogeny broth (LB) medium (0.5% yeast extract, 1% tryptone, 0.5% NaCl) supplemented as required with ampicillin (100 µg/ml). Solid medium was prepared by adding 2% agar to LB medium.

The yeast strains used in this study are listed in Table S3. *S. cerevisiae*, *C. boidinii*, and *P. pastoris* cells were grown on yeast extract peptone dextrose (YPD) medium (1% Bacto-yeast extract, 2% Bacto-peptone, 2% glucose), synthetic defined (SD) medium (0.67% Yeast Nitrogen Base without aa, 2% glucose), or SD-Trp medium (SD medium supplemented with 1.92 g/l yeast synthetic drop-out medium supplements without tryptophan; Sigma-Aldrich). The pH of SD medium was adjusted to 6.0 with NaOH. For selection of strain *Cbhog1*Δ (*ura3*), 2.4 µg/ml of uracil or 0.08% w/v of 5-fluoroorotidic acid (5-FOA) was added to SD medium. *S. pombe* cells were grown on YES medium (0.5% Bacto-yeast extract, 3% glucose, 75 mg/l adenine, leucine, uracil and lysine). Cultivation was performed at 28°C under aerobic conditions, and cell growth was monitored by measuring the optical density of the medium at OD_{610}. Solid media were prepared by adding 2% agar to the appropriate liquid media. The *Spsty1*Δ strain expressing Sty1-GFP (FY14931) was provided by the NBRP (YGRC), Japan.

DNA isolation and transformation

Plasmid DNAs from *E. coli* were isolated using Wizard Plus SV Minipreps DNA Purification System (Promega, Madison, WI). Transformation of

Journal of Cell Science (2018) 131, jcs209114. doi:10.1242/jcs.209114

E. coli was performed by the method of Dower et al. (1988). Yeast DNA was isolated by the method of Cryer et al. (1975). Transformation of *S. cerevisiae* was performed using the Fast yeast transformation kit (G-Biosciences, Maryland Heights, MO). Transformation of *C. boidinii* was performed using a modified version of the lithium acetate method (Sakai and Tani, 1992). Transformation of *P. pastoris* was performed as described previously (Higgins and Cregg, 1998).

Plasmid construction for expression in *C. boidinii*

The oligonucleotide primers used for PCR reactions are listed in Table S4. The plasmids used in this study are listed in Table S5. A deletion cassette for the *CbHOG1* gene was constructed as follows: Primers CbHOG1_UP_Fw and CbHOG1_UP_Rv were used to amplify a 1.0-kb fragment, using genomic DNA of *C. boidinii* as template. The PCR product was fused with the 7.6-kb *Kpn*I-digested fragment of pSK+SPR using the In-fusion HD cloning kit (TaKaRa, Kyoto, Japan), yielding pHC100. Then, primers CbHOG1_DOWN_Fw and CbHOG1_DOWN_Rv were used to amplify a second 1.0-kb fragment, using genomic DNA of *C. boidinii* as template. The PCR product was fused with the 8.6-kb *Sac*I-digested fragment of pHC100 using the In-fusion HD cloning kit, yielding the *CbHOG1* disruption vector pHC101.

The *CbHOG1* promoter and ORF region without the STOP codon were amplified with primers CbHOG1_Vn_Fw and CbHOG1_Vn_Rv, using genomic DNA of *C. boidinii* as template. The PCR product was fused with the 6.4-kb *Afl*III–*Sal*I fragment of plasmids pKK001 and pSPM001 using the In-fusion HD cloning kit, yielding pHC200 and pHC400, respectively. The *ScHOG1* ORF region without the STOP codon was amplified with primers P_{CbACT1}ScHOG1_Vn_Fw and P_{CbACT1}ScHOG1_Vn_Rv. The PCR product was fused with the 8.1-kb *Sal*I-digested fragment of pKK001 using the In-fusion HD cloning kit, yielding pHC300. The *CbPAB1* promoter and ORF region without the STOP codon were amplified with primers CbPab1_Fw and CbPab1_Rv, using genomic DNA of *C. boidinii* as template. The PCR product was fused with the 6.4-kb *Afl*III–*Sal*I fragment of plasmid pKK001 using the In-fusion HD cloning kit, yielding pHC401. pHC404 was constructed in a similar manner, with primers CbEdc3_Fw and CbEdc3_Rv. The *CbPBP1* promoter and ORF region without the STOP codon were amplified with primers CbPbp1_Fw and CbPbp1_Rv, using genomic DNA of *C. boidinii* as template. The PCR product was fused with the 6.4-kb *Afl*III–*Sal*I fragment of plasmid pSPM001 using the In-fusion HD cloning kit, yielding pHC403. Vector pHC402, encoding CbPab1-Venus under the control of the *PAB1* promoter with the *LEU2* marker (Sakai and Tani, 1992) was constructed by ligation of an *Aat*II–*Nar*I fragment from pHC401 with an *Aat*II–*Nar*I fragment of the *LEU2* gene. Vector pHC405 was constructed in a similar manner from pHC404.

C. boidinii strains expressing truncated variants of CbHog1 were constructed using the plasmids pHC200-pHC213, which were transformed into *Cbhog1Dura3*. pHC201, a deletion mutant of *CbHOG1*, was constructed as follows: Primers CbHOG1_Vn_Δ(1-10)_Fw and CbHOG1_Vn_ΔN_Rv were phosphorylated at their 5′-ends with T4 nucleotide kinase, and used to amplify an 8.6-kb fragment by inverse PCR using pHC200 as template. The PCR product was self-ligated, yielding vector pHC201. Other deletion mutants of *CbHOG1* were constructed in a similar way with primer sets CbHOG1_Vn_Δ(1-17)_Fw/CbHOG1_Vn_ΔN_Rv, CbHOG1_Vn_Δ(1-20)_Fw/CbHOG1_Vn_ΔN_Rv, CbHOG1_Vn_Δ(1-30)_Fw/CbHOG1_Vn_ΔN_Rv, CbHOG1_Vn_Δ(1-41)_Fw/CbHOG1_Vn_ΔN_Rv, HOG1_Vn_ΔC_Fw/CbHOG1_Vn_Δ(348-398)_Rv, HOG1_Vn_ΔC_Fw/CbHOG1_Vn_Δ(318-398)_Rv, HOG1_Vn_ΔC_Fw/CbHOG1_Vn_Δ(300-398)_Rv, HOG1_Vn_ΔC_Fw/CbHOG1_Vn_(1-20)_Rv, HOG1_Vn_ΔC_Fw/CbHOG1_Vn_(1-30)_Rv, HOG1_Vn_ΔC_Fw/CbHOG1_Vn_(1-40)_Rv, HOG1_Vn_ΔC_Fw/CbHOG1_Vn_(1-50)_Rv, and HOG1_Vn_ΔC_Fw/CbHOG1_Vn_(346-398)_Rv, yielding vectors pHC202, pHC203, pHC204, pHC205, pHC206, pHC207, pHC208, pHC209, pHC210, pHC211, pHC212, and pHC213, respectively. Deletion mutants of ScHOG1 were also constructed in a similar manner. The 1.6-kb *Sal*I–*Eco*RI fragment of plasmid pSPM001 and the 4.1-kb *Sal*I–*Eco*RI fragment of plasmid pHC200 were ligated, yielding vector pHC400.

C. boidinii strains expressing other series of truncated variants of CbHog1 were constructed using the plasmids pHC214-pHC221, which were transformed into *Cbhog1Dura3*. pHC214, a deletion mutant of *CbHOG1*, was constructed as follows. The *CbHOG1* promoter and ORF region were amplified with primers CbHOG1_Vn_Δ(25-28)_Fw and CbHOG1_Vn_Δ(25-28)_Rv, using genomic DNA of *C. boidinii* as template. The PCR product was purified using the NucleoSpin Gel and PCR Clean-up kit and directly transformed into *E. coli* DH10B. The fragment was circularized in the host cells, yielding vector pHC214. Additional deletion mutants of CbHOG1 were constructed in a similar manner using primer sets CbHOG1_Vn_Δ(35-40)_Fw/CbHOG1_Vn_Δ(35-40)_Rv, CbHOG1_Vn_Δ(38-45)_Fw/CbHOG1_Vn_Δ(38-45)_Rv, CbHOG1_Vn_Δ(39-45)_Fw/CbHOG1_Vn_Δ(39-45)_Rv, CbHOG1_Vn_Δ(40-45)_Fw/CbHOG1_Vn_Δ(40-45)_Rv, CbHOG1_Vn_Δ(43-45)_Fw/CbHOG1_Vn_Δ(43-45)_Rv, and CbHOG1_Vn_Δ(K50R)_Fw/CbHOG1_Vn_Δ(K50R)_Rv, yielding vectors pHC215, pHC216, pHC217, pHC218, pHC219, and pHC220, respectively. Vector pHC221, encoding CbHog1 (K50R)-mCherry under the control of the *HOG1* promoter with the *LEU2* marker, was constructed by ligation of an *Aat*II–*Nar*I fragment of pHC220 with an *Aat*II–*Nar*I fragment of the *LEU2* gene.

C. boidinii strains expressing variant ScHog1 were constructed using the plasmids pHC500-pHC504, which were transformed into *Cbhog1Dura3*. pHC501, encoding a kinase-inactive form of *ScHOG1*, was constructed as follows. Primers ScHOG1_KD_Fw and ScHOG1_KD_Rv were phosphorylated at their 5′-ends with T4 nucleotide kinase, and used to amplify an 8.6-kb fragment by inverse PCR using plasmid pHC500 as template. The PCR product was self-ligated, yielding vector pHC501. Other plasmids harboring mutated ScHOG1 were constructed in a similar way using primer sets ScHOG1_nP_Fw/ScHOG1_nP_Fw and ScHOG1_CAAX_Fw/ScHOG1_CAAX_Rv, yielding vectors pHC502, and pHC503, respectively. pHC504 was constructed as follows. Primers HOG1_Vn_ΔC_Fw and ScHOG1_350_Rv were phosphorylated at their 5′-ends with T4 nucleotide kinase, and used to amplify an 8.3-kb fragment by inverse PCR using plasmid pHC300 as template. The PCR product was self-ligated, yielding vector pHC504.

The *C. boidinii* strain expressing CbHog1-ScHog1(351-435) was constructed using the plasmid pHC505, which was transformed into *Cbhog1Dura3*. pHC505, encoding *CbHOG1* and the C-terminal region of *ScHOG1*, was constructed as follows. The *CbHOG1* promoter and ORF region were amplified with primers CbHOG1_Vn_(1-398)_Fw and CbHOG1_Vn_(1-398)_Rv, using the plasmid pHC200 as template. The C-terminal region of *ScHOG1* was amplified with primers ScHog1_(351-435)_Fw and ScHog1_(351-435)_Rv, using the plasmid pHC300 as template. Those two fragments were fused using the In-fusion HD cloning kit, yielding pHC505.

CbHOG1 gene disruption

A deletion cassette for the *CbHOG1* gene was amplified with CbHOG1_SPR_Fw/CbHOG1_SPR_Rv, using plasmid pHC101 as template. The PCR product was transformed into *C. boidinii* TK62 using a modified version of the lithium acetate method (Sakai and Tani, 1992). Proper gene disruption was confirmed by colony PCR. The constructed *Cbhog1*Δ strain was converted to uracil auxotrophy by 5-FOA selection, yielding the *Cbhog1*Δ*ura3* strain. Restoration of the marker gene *URA3* was confirmed by PCR analysis. The nucleotide sequence of *CbHOG1* was deposited in DNA Data Bank of Japan (DDBJ) under the accession number LC312444. The nucleotide sequences of *CbPAB1*, *CbPBP1* and *CbEDC3* were also deposited in DDBJ under accession numbers, LC312445, LC312446, and LC312447, respectively.

Vectors and plasmids for *S. cerevisiae*

The oligonucleotide primers used for PCR reactions are listed in Table S4. The plasmids used in this study are listed in Table S5. The *S. cerevisiae* strain expressing ScHog1-GFP was constructed as follows: the GFP-LEU2 region was PCR-amplified with primers ScHOG1CTag_Fw and ScHog1CTag_Rv, using vector pMO152 as template. The fragment containing the GFP-LEU2 gene was directly integrated into the C-

terminal region of the *ScHOG1* gene, yielding a *S. cerevisiae* strain expressing ScHog1-GFP.

Vectors and plasmids for *P. pastoris*

The oligonucleotide primers used for PCR reactions are listed in Table S4. The plasmids used in this study are listed in Table S5. The deletion strain of the *PpHOG1* gene was constructed as follows. Deletion cassettes were amplified with primers Zhog1_UPfw/Zhog1_UPrv and Zhog1_DWfw/Zhog1_DWrv, using genomic DNA of *P. pastoris* as template. The PCR products were linked by PCR with primers Zhog1_UPfw and Zhog1_DWrv, yielding a 2.0-kb fragment containing the upstream and downstream regions of the *PpHOG1* gene. The zeocin resistance marker, which was used for the selection of disruptants of the *PpHOG1* gene, was PCR-amplified using vector pPICZ A as template, yielding a 1.9-kb fragment. These two fragments were fused using the In-fusion HD cloning kit, yielding *PpHOG1* disruption vector pHP001. pHP001 vector was linearized with *Xba*I and transformed into the host strain PPY12. Proper gene disruption was confirmed by colony PCR.

The vector harboring PpHog1-YFP was constructed as follows. The *PpHOG1* promoter and the ORF region without the STOP codon were amplified using primers PpHog1IF_fw and PpHog1IF_rv, using genomic DNA of *P. pastoris* as template. The PCR product was fused with the 3.4-kb *Bam*HI–*Spe*I fragment of plasmid pNT204 using the In-fusion HD cloning kit, yielding pHP100. Vector pHP100 was linearized with *Xba*I and transformed into the *PpHOG1* deletion (*Pphog1*Δ) host strain.

Analysis of intracellular localization of fluorescent proteins under hyperosmotic stress condition

Yeast cells were pre-cultured to stationary phase at 28°C in 5 ml YPD (for *S. cerevisiae*, *C. boidinii* or *P. pastoris*) medium or YES (for *S. pombe*) medium. Subsequently, 20-µl aliquots of the cultures were transferred to 5 ml SD-Trp (for *S. cerevisiae*), SD (for *C. boidinii* or *P. pastoris*), or YES (for *S. pombe*) medium, and the cells were grown to early-log phase at 28°C. The cultures were centrifuged at 6000 rpm for 2 min, and cells were transferred to 5 ml fresh SD-Trp medium containing 0.5 M NaCl (for *S. cerevisiae*), SD medium containing 0.4 M NaCl (for *C. boidinii*), SD medium containing 0.5 M NaCl (for *P. pastoris*), or YES medium containing 1 M KCl (for *S. pombe*) at 28°C for 5 min (for *S. cerevisiae*, *C. boidinii* or *P. pastoris*) or 10 min (for *S. pombe*). The cells were then harvested by centrifugation for microscopic observation.

Analysis of intracellular localization of fluorescent proteins under high-temperature stress

Yeast cells were pre-cultured to the stationary phase at 28°C in 5 ml YPD (for *S. cerevisiae*, *C. boidinii*, or *P. pastoris*) or YES (for *S. pombe*) medium. Subsequently, 20-µl aliquots of these cultures were transferred to 5 ml SD-Trp (for *S. cerevisiae*), SD (for *C. boidinii* or *P. pastoris*), or YES (for *S. pombe*) medium, and the cells were grown to early-log phase at 28°C. The cells were then subjected to the indicated high-temperature stresses, and harvested by centrifugation for microscopic observation.

Nuclear staining

After cell cultivation for the indicated time period, sample cells were harvested, washed once and fixed with 1 ml of 70% ethanol for 30 min at room temperature. Fixed cells were then washed twice, resuspended in 150 µl of sterilized water, and stained with 150 µl of 0.125 µg/ml DAPI (4′, 6′-diamidino-2-phenylindole) solution. After 10 min of incubation, samples were used for microscopic observation.

Fluorescence microscopy

Fluorescence microscopy was performed using an IX81 inverted microscope (Olympus) equipped with an UPLAN-Apochromat 100×/1.35 NA oil iris objective lens. Venus and mCherry signals were acquired using a Plan Fluor 100×lens (Carl Zeiss) with pinhole set to 1.02 airy units for YFP acquisition. Images were analyzed using the METAMORPH imaging software (Molecular Devices) and Adobe Photoshop CS6 (Adobe). All scale bars shown in microscope photographs are 2 µm. Fluorescence observations of cells cultured *in vitro* were repeated at least twice, and three images of different fields were acquired at each time point.

Morphometric analysis

Cells (>50 per field) were counted in at least three fluorescence microscope fields, and independent observations were repeated at least three times.

Preparation of cell samples for immunoblot analysis

To prepare samples for Phos-tag SDS-PAGE, harvested cells were suspended in lysis buffer (0.2 N NaOH, 1% [v/v] 2-mercaptoethanol) and incubated at 4°C for 10 min. Next, trichloroacetic acid was added (final concentration 10%). Then, the samples were vortexed, incubated at 4°C for 10 min and centrifuged. Subsequently, the pellet was washed twice with acetone and resuspended in sample buffer (16.7 mM Tris-HCl pH 6.8, 1% SDS, 10% Glycerol, 1% 2-mercaptoethanol, 1 mM $MnCl_2$) and boiled for 3 min.

SDS-PAGE with or without Phos-tag and immunoblot analysis

The prepared samples were electrophoresed on a 6% Phos-tag SDS polyacrylamide gel (containing 30 µM Phos-tag [Wako], 100 µM $MnCl_2$) or 10% normal SDS polyacrylamide gel. Western analysis was performed by the method of Towbin et al. (Towbin et al., 1979). The proteins on a gel were transferred to a PROTRAN nitrocellulose transfer membrane (Schleicher & Schuell BioScience, Inc., Dassel, Germany) in a tank blotting system (BIO-RAD) at 100 V for 1 h. After the transfer, the membrane was blocked for 1 h in TBS-T buffer (0.3% Tris, 0.8% NaCl, 0.02% KCl, 0.1% Tween 20 pH 8.0) supplemented with 5% skimmed milk. The blots were then incubated for 1 h with monoclonal anti-GFP antibody (Clontech, cat. no. 632381) at 1:1000 dilution in TBS-T buffer, and washed three times with TBS-T. Subsequently, the blots were incubated for 1 h with an anti-mouse IgG (MBL, cat. no. 330) at 1:10,000 dilution in TBS-T, and washed three times in TBS-T. Immunoreactive bands were visualized using the Western Lightning Chemiluminescence Reagent Plus (Perkin-Elmer Life Science), and the signals were detected on a Light-Capture II (ATTO).

Competing interests

The authors declare no competing or financial interests.

Author contributions

Conceptualization: K.S., T.H., H.Y., Y.S.; Investigation: K.S., T.H., A.H.; Writing - original draft: K.S., T.H.; Writing - review & editing: H.Y., Y.S.; Supervision: H.Y., Y.S.; Project administration: Y.S.; Funding acquisition: K.S., H.Y., Y.S.

Funding

K.S. is a Research Fellow of Japan Society for the Promotion of Science (JSPS). This research was supported in part by a Grant-in-Aid for JSPS Research Fellows [grant number: 16J10395 to K.S.] and Grant-in-Aid for Challenging Exploratory Research [grant numbers: 16K14883 (to Y.S.) and 16K15089 (to H.Y.)] from the JSPS. This study was partly supported by the Program for Leading Graduate Schools (all-round model) from the Ministry of Education, Culture, Sports, Science and Technology, Japan (to K.S.).

Data availability

The nucleotide sequences of *CbHOG1*, *CbPAB1*, *CbPBP1* and *CbEDC3* were deposited in the DNA Data Bank of Japan (DDBJ) under accession numbers LC312444, LC312445, LC312446, and LC312447, respectively.

Supplementary information

Supplementary information available online at
http://jcs.biologists.org/lookup/doi/10.1242/jcs.209114.supplemental

References

Arimoto, K., Fukuda, H., Imajoh-Ohmi, S., Saito, H. and Takekawa, M. (2008). Formation of stress granules inhibits apoptosis by suppressing stress-responsive MAPK pathways. *Nat. Cell Biol.* **10**, 1324-1332.

Bentmann, E., Neumann, M., Tahirovic, S., Rodde, R., Dormann, D. and Haass, C. (2012). Requirements for stress granule recruitment of fused in sarcoma (FUS)

and TAR DNA-binding protein of 43 kDa (TDP-43). *J. Biol. Chem.* **287**, 23079-23094.
Borbolis, F. and Syntichaki, P. (2015). Cytoplasmic mRNA turnover and ageing. *Mech. Ageing Dev.* **152**, 32-42.
Brengues, M., Teixeira, D. and Parker, R. (2005). Movement of eukaryotic mRNAs between polysomes and cytoplasmic processing bodies. *Science* **310**, 486-489.
Brewster, J. L. and Gustin, M. C. (2014). Hog1: 20 years of discovery and impact. *Sci. Signal.* **7**, re7.
Brewster, J. L., de Valoir, T., Dwyer, N. D., Winter, E. and Gustin, M. C. (1993). An osmosensing signal transduction pathway in yeast. *Science* **259**, 1760-1763.
Buchan, J. R. and Parker, R. (2009). Eukaryotic stress granules: the ins and outs of translation. *Mol. Cell* **36**, 932-941.
Buchan, J. R., Yoon, J.-H. and Parker, R. (2011). Stress-specific composition, assembly and kinetics of stress granules in *Saccharomyces cerevisiae*. *J. Cell Sci.* **124**, 228-239.
Casey, P. J., Solski, P. A., Der, C. J. and Buss, J. E. (1989). p21ras is modified by a farnesyl isoprenoid. *Proc. Natl. Acad. Sci. USA* **86**, 8323-8327.
Cobb, M. H. and Goldsmith, E. J. (1995). How MAP kinases are regulated. *J. Biol. Chem.* **270**, 14843-14846.
Cryer, D. R., Eccleshall, R. and Marmur, J. (1975). Isolation of yeast DNA. *Methods Cell Biol.* **12**, 39-44.
Demetriades, C., Doumpas, N. and Teleman, A. A. (2014). Regulation of TORC1 in response to amino acid starvation via lysosomal recruitment of TSC2. *Cell* **156**, 786-799.
Deschenes, R. J., Stimmel, J. B., Clarke, S., Stock, J. and Broach, J. R. (1989). *RAS2* protein of *Saccharomyces cerevisiae* is methyl-esterified at its carboxyl terminus. *J. Biol. Chem.* **264**, 11865-11873.
Dower, W. J., Miller, J. F. and Ragsdale, C. W. (1988). High efficiency transformation of *E. coli* by high voltage electroporation. *Nucleic Acids Res.* **16**, 6127-6145.
Ferrigno, P., Posas, F., Koepp, D., Saito, H. and Silver, P. A. (1998). Regulated nucleo/cytoplasmic exchange of HOG1 MAPK requires the importin beta homologs NMD5 and XPO1. *EMBO J.* **17**, 5606-5614.
Hall, J. P., Cherkasova, V., Elion, E., Gustin, M. C. and Winter, E. (1996). The osmoregulatory pathway represses mating pathway activity in *Saccharomyces cerevisiae*: isolation of a *FUS3* mutant that is insensitive to the repression mechanism. *Mol. Cell. Biol.* **16**, 6715-6723.
Hancock, J. F., Paterson, H. and Marshall, C. J. (1990). A polybasic domain or palmitoylation is required in addition to the CAAX motif to localize p21ras to the plasma membrane. *Cell* **63**, 133-139.
Herskowitz, I. (1995). MAP kinase pathways in yeast: for mating and more. *Cell* **80**, 187-197.
Higa, M., Kita, A., Hagihara, K., Kitai, Y., Doi, A., Nagasoko, R., Satoh, R. and Sugiura, R. (2015). Spatial control of calcineurin in response to heat shock in fission yeast. *Genes Cells* **20**, 95-107.
Higgins, D. R. and Cregg, J. M. (1998). *Pichia Protocols*. Totowa, NJ: Humana Press.
Hohmann, S. (2002). Osmotic stress signaling and osmoadaptation in yeasts. *Microbiol. Mol. Biol. Rev.* **66**, 300-372.
Horvitz, H. R. and Sternberg, P. W. (1991). Multiple intercellular signalling systems control the development of the *Caenorhabditis elegans* vulva. *Nature* **351**, 535-541.
Kato, K., Yamamoto, Y. and Izawa, S. (2011). Severe ethanol stress induces assembly of stress granules in *Saccharomyces cerevisiae*. *Yeast* **28**, 339-347.
Kawaguchi, K., Yurimoto, H., Oku, M. and Sakai, Y. (2011). Yeast methylotrophy and autophagy in a methanol-oscillating environment on growing *Arabidopsis thaliana* leaves. *PLoS ONE* **6**, e25257.
Kedersha, N., Stoecklin, G., Ayodele, M., Yacono, P., Lykke-Andersen, J., Fritzler, M. J., Scheuner, D., Kaufman, R. J., Golan, D. E. and Anderson, P. (2005). Stress granules and processing bodies are dynamically linked sites of mRNP remodeling. *J. Cell Biol.* **169**, 871-884.
Kim, W. J., Back, S. H., Kim, V., Ryu, I. and Jang, S. K. (2005). Sequestration of TRAF2 into stress granules interrupts tumor necrosis factor signaling under stress conditions. *Mol. Cell. Biol.* **25**, 2450-2462.
Millar, J. B., Buck, V. and Wilkinson, M. G. (1995). Pyp1 and Pyp2 PTPases dephosphorylate an osmosensing MAP kinase controlling cell size at division in fission yeast. *Genes Dev.* **9**, 2117-2130.
Morano, K. A., Grant, C. M. and Moye-Rowley, W. S. (2012). The response to heat shock and oxidative stress in *Saccharomyces cerevisiae*. *Genetics* **190**, 1157-1195.
Murakami, Y., Tatebayashi, K. and Saito, H. (2008). Two adjacent docking sites in the yeast Hog1 mitogen-activated protein (MAP) kinase differentially interact with the Pbs2 MAP kinase kinase and the Ptp2 protein tyrosine phosphatase. *Mol. Cell. Biol.* **28**, 2481-2494.
Nilsson, D. and Sunnerhagen, P. (2011). Cellular stress induces cytoplasmic RNA granules in fission yeast. *RNA* **17**, 120-133.
Sakai, Y. and Tani, Y. (1992). Directed mutagenesis in an asporogenous methylotrophic yeast: cloning, sequencing, and one-step gene disruption of the 3-isopropylmalate dehydrogenase gene (*LEU2*) of *Candida boidinii* to derive doubly auxotrophic marker strains. *J. Bacteriol.* **174**, 5988-5993.
Shiraishi, K., Oku, M., Kawaguchi, K., Uchida, D., Yurimoto, H. and Sakai, Y. (2015). Yeast nitrogen utilization in the phyllosphere during plant lifespan under regulation of autophagy. *Sci. Rep.* **5**, 9719.
Takahara, T. and Maeda, T. (2012). Transient sequestration of TORC1 into stress granules during heat stress. *Mol. Cell* **47**, 242-252.
Towbin, H., Staehelin, T. and Gordon, J. (1979). Electrophoretic transfer of proteins from polyacrylamide gels to nitrocellulose sheets: procedure and some applications. *Proc. Natl. Acad. Sci. USA* **76**, 4350-4354.
Weissbach, R. and Scadden, A. D. J. (2012). Tudor-SN and ADAR1 are components of cytoplasmic stress granules. *RNA* **18**, 462-471.
Winkler, A., Arkind, C., Mattison, C. P., Burkholder, A., Knoche, K. and Ota, I. (2002). Heat stress activates the yeast high-osmolarity glycerol mitogen-activated protein kinase pathway, and protein tyrosine phosphatases are essential under heat stress. *Eukaryot. Cell* **1**, 163-173.

Table S1. Comparison of amino acid sequences of P-body and SG components in *C. boidinii* with those in *S. cerevisiae.*

	protein	identity (%)	similarity (%)
P-body components	Edc3	25	57
SG components	Pab1	56	76
	Pbp1	23	55

Journal of Cell Science • Supplementary information

Table S2. Intracellular localization of CbHog1-mCherry and CbEdc3-Venus derived from quantification of 50 cells after high temperature stress for 30 min.

	Dot number / 50 cells
Colocalized	43.3 ± 4.0
CbHog1-mCherry only	248.0 ± 10.5
Pab1-Venus only	113.7 ± 6.0

Errors represent the S.D. of triplicate measurements.

Journal of Cell Science • Supplementary information

Table S3. Yeast strains used in this study.

Strain	Genotype	Reference
S. cerevisiae		
BY4741	MATa *his3Δ1 leu2Δ0 met15Δ0 ura3Δ0*	(Brachmann et al., 1998)
HS01	BY4741, *Schog1*::*ScHOG1-GFP, LEU2*	This study
HS02	BY4741, (P_{ScHOG1}*CbHOG1-Venus, LEU2*	This study
HS03	BY4741, *Schog1*::*ScHOG1(1-350)-Venus, LEU2*	This study
C. boidinii		
AOU1	Wild type	(Tani et al., 1985)
TK62	*ura3*	(Sakai et al., 1991)
HC01	TK62, *Cbhog1Δ*::*URA3*	This study
HC02	HC01, *ura3*	This study
HC03	HC02, *ura3*::(P_{CbHOG1}*CbHOG1-Venus, URA3*)	This study
HC04	HC02, *ura3*::(P_{CbACT1}*ScHOG1-Venus, URA3*)	This study
HC05	HC02, *ura3*::(P_{CbHOG1}*CbHOG1Δ(1-10)-Venus, URA3*)	This study
HC06	HC02, *ura3*::(P_{CbHOG1}*CbHOG1Δ(1-17)-Venus, URA3*)	This study
HC07	HC02, *ura3*::(P_{CbHOG1}*CbHOG1Δ(1-20)-Venus, URA3*)	This study
HC08	HC02, *ura3*::(P_{CbHOG1}*CbHOG1Δ(1-30)-Venus, URA3*)	This study
HC09	HC02, *ura3*::(P_{CbHOG1}*CbHOG1Δ(1-41)-Venus, URA3*)	This study
HC10	HC02, *ura3*::(P_{CbHOG1}*CbHOG1Δ(348-398)-Venus, URA3*)	This study
HC11	HC02, *ura3*::(P_{CbHOG1}*CbHOG1Δ(318-398)-Venus, URA3*)	This study
HC12	HC02, *ura3*::(P_{CbHOG1}*CbHOG1Δ(300-398)-Venus, URA3*)	This study
HC13	HC02, *ura3*::(P_{CbHOG1}*CbHOG1(1-20)-Venus, URA3*)	This study
HC14	HC02, *ura3*::(P_{CbHOG1}*CbHOG1(1-30)-Venus, URA3*)	This study
HC15	HC02, *ura3*::(P_{CbHOG1}*CbHOG1(1-40)-Venus, URA3*)	This study
HC16	HC02, *ura3*::(P_{CbHOG1}*CbHOG1(1-50)-Venus, URA3*)	This study
HC17	HC02, *ura3*::(P_{CbHOG1}*CbHOG1(346-398)-Venus, URA3*)	This study
HC18	HC02, *ura3*::(P_{CbHOG1}*CbHOG1Δ(25-28)-Venus, URA3*)	This study
HC19	HC02, *ura3*::(P_{CbHOG1}*CbHOG1Δ(35-40)-Venus, URA3*)	This study
HC20	HC02, *ura3*::(P_{CbHOG1}*CbHOG1Δ(38-45)-Venus, URA3*)	This study
HC21	HC02, *ura3*::(P_{CbHOG1}*CbHOG1Δ(39-45)-Venus, URA3*)	This study
HC22	HC02, *ura3*::(P_{CbHOG1}*CbHOG1Δ(40-45)-Venus, URA3*)	This study
HC23	HC02, *ura3*::(P_{CbHOG1}*CbHOG1Δ(43-45)-Venus, URA3*)	This study
HC24	HC02, *ura3*::(P_{CbACT1}*ScHOG1-K52R-Venus, URA3*)	This study
HC25	HC02, *ura3*::(P_{CbACT1}*ScHOG1-T174A/Y176F-Venus, URA3*)	This study
HC26	HC02, *ura3*::(P_{CbACT1}*ScHOG1 Venus-CAAXRas2, URA3*)	This study
HC27	HC02, *ura3*::(P_{CbACT1}*ScHOG1(1-350)-Venus, URA3*)	This study
HC28	HC02, ura3::(P_{CbHOG1}*CbHOG1-Sc(351-435)-Venus, URA3*)	This study
BUL	*ura3*, *leu2*	(Sakai and Tani 1992)
SK01	BUL, *leu2*::(P_{CbPAB1}*CbPAB1-Venus, LEU2*), *ura3*::(P_{CbPBP1}*CbPBP1-mCherry, URA3*)	This study
HC30	BUL, *leu2*::(P_{CbPAB1}*CbPAB1-Venus, LEU2*), *ura3*::(P_{CbHOG1}*CbHOG1-mCherry, URA3*)	This study
HC31	HC02, *ura3*::(P_{CbHOG1}*CbHOG1(K50R)-Venus, URA3*)	This study
HC32	BUL, *leu2*::(P_{CbPAB1}*CbPAB1-Venus, LEU2*), *ura3*::(P_{CbHOG1}*CbHOG1(K50R)-mCherry, URA3*)	This study
HC33	HC02, *ura3*::(P_{CbEDC3}*CbEDC3-Venus, URA3*)	This study
HC34	BUL, *leu2*::(P_{CbEDC3}*CbEDC3-Venus, LEU2*), *ura3*::(P_{CbHOG1}*CbHOG1(K50R)-mCherry, URA3*)	This study
HC35	HC02, *ura3*::(P_{CbPAB1}*CbPAB1-Venus, URA3*)	This study
P. pastoris		
PPY12	*arg4 his4*	(Sakai et al., 1998)
HP01	PPY12, *Pphog1Δ*::*Zeo*^{r}	This study
HP02	HP01, *arg4*::(P_{PpHOG1}*PpHOG1-YFP, ARG4*)	This study
S. pombe		
FY14931	*ade6-216 leu1-32 lys1-131 ura4-D18 sty1*::*sty1-GFP-HA*, *Kan*^{r}	Purchased from NBRP

Journal of Cell Science • Supplementary information

Table S4. Primers used in this study.

Designation	DNA sequence (5' → 3')
CbHOG1_UP_Fw	GGGCGAATTGGGTACGGCGCCGATGGAAATATGGAAACAGAGATG
CbHOG1_UP_Rv	GGGGGGGCCCGGTACCACCCATACCAACTGGATTTAAA
CbHOG1_DOWN_Fw	CACCGCGGTGGAGCTCAACAACAGCTGTAACAATAATTCAAG
CbHOG1_DOWN_Rv	ACAAAAGCTGGAGCTGAATTCCAACATGTCCAACAACAACAAC
CbHOG1_SPR_Fw	GATGGAAATATGGAAACAGAGATG
CbHOG1_SPR_Rv	CAACATGTCCAACAACAACAAC
CbHOG1_Vn_Fw	CTTTTGCTCACATGTGATGGAAATATGGAAACAGAGATGAAG
CbHOG1_Vn_Rv	AGAAACCATGTCGACCAGCTGTTGTTGTTGTTGTTGTT
P_{CbACT1}ScHOG1_Vn_Fw	ATATTACAAAAGTCGACATGACCACTAACGAGGAATTCATTAG
P_{CbACT1}ScHOG1_Vn_Rv	TTAGAAACCATGTCGACCTGTTGGAACTCATTAGCGTACTG
CbHOG1_Vn_Δ(1-10)_Fw	TTTGGTACTATATTTGAAACAACAAATAGATACTC
CbHOG1_Vn_Δ(1-17)_Fw	ACAAATAGATACTCAGATTTAAATCCAG
CbHOG1_Vn_Δ(1-20)_Fw	TACTCAGATTTAAATCCAGTTGGTATGG
CbHOG1_Vn_Δ(1-30)_Fw	GCATTTGGTTTAGTTTGTGCAGC
CbHOG1_Vn_Δ(1-41)_Fw	TTAACAAATCAAAATGTTGCAATTAAAAAAGTTATGAAACCTTTTTC
CbHOG1_Vn_Δ(348-398)_Rv	TTCAACTTGATGGAAATCTAAGATTTCAC
CbHOG1_Vn_Δ(318-398)_Rv	ATCGAATTTTTCTTCAGCAACTGGTTC
CbHOG1_Vn_Δ(300-398)_Rv	GTATTCATGTTCTAAAGCTTGTTCTGC
CbHOG1_Vn_ΔN_Rv	CATTTTATTTATATCTATATATATATATGTCTATTGTATATGTCTATTGTC
HOG1_Vn_ΔC_Fw	GTCGACATGGTTTCTAAAGGTG
CbHOG1_Vn_(1-20)_Rv	TCTATTTGTTGTTTCAAATATAGTACCAAATATTTGAGTTC
CbHOG1_Vn_(1-30)_Rv	ACCCATACCAACTGGATTTAAATCTG
CbHOG1_Vn_(1-40)_Rv	ATCCTTTGCTGCACAAACTAAACC
CbHOG1_Vn_(1-50)_Rv	TTTAATTGCAACATTTTGATTTGTTAATTTATCCTTTGC
CbHOG1_Vn_(346-398)_Rv	GGTGCTGAAGCTGATGCTTTA
CbHOG1_Vn_Δ(25-28)_Fw	AGATTTAATGGGTGCATTTGGTTTAGTTTG
CbHOG1_Vn_Δ(25-28)_Rv	TGCACCCATTAAATCTGAGTATCTATTTGTTGTTTCAAATATAGTAC
CbHOG1_Vn_Δ(35-40)_Fw	TGGTTTAAAATTAACAAATCAAAATGTTGCAATTAAAAAAGTTATGAA
CbHOG1_Vn_Δ(35-40)_Rv	GTTAATTTTAAACCAAATGCACCCATACCAA
CbHOG1_Vn_Δ(38-45)_Fw	TTGTGCAAATGTTGCAATTAAAAAAGTTATGAAACCTTTTTCA
CbHOG1_Vn_Δ(38-45)_Rv	GCAACATTTGCACAAACTAAACCAAATGCAC
CbHOG1_Vn_Δ(39-45)_Fw	TGCAGCAAATGTTGCAATTAAAAAAGTTATGAAACCTTTTTCA
CbHOG1_Vn_Δ(39-45)_Rv	GCAACATTTGCTGCACAAACTAAACCAAATG
CbHOG1_Vn_Δ(40-45)_Fw	GCAGCAAAGAATGTTGCAATTAAAAAAGTTATGAAACCTTTTTCAA
CbHOG1_Vn_Δ(40-45)_Rv	GCAACATTCTTTGCTGCACAAACTAAACCAAAT
CbHOG1_Vn_Δ(43-45)_Fw	TAAATTAAATGTTGCAATTAAAAAAGTTATGAAACCTTTTTCAA
CbHOG1_Vn_Δ(43-45)_Rv	GCAACATTTAATTTATCCTTTGCTGCACAAACTAAAC
CbHOG1_Vn_(K50R)_Fw	GCAATTAAAAAAGTTATGAAACCTTTTTCAACTGCTGTATTAG
CbHOG1_Vn_(K50R)_Rv	AACTTTTTTAATTGCAACTGGCTGCACAAACTAAAC
CbHOG1_Vn_(1-398)_Fw	CTGCAGGGAATTTAATCATTTTCAA
CbHOG1_Vn_(1-398)_Rv	CAGCTGTTGTTGTTGTTGTT
CbPab1_Fw	CTTTTGCTCACATGTGGCGCTTAATTTTGGCTGAATC
CbPab1_Rv	AGAAACCATGTCGACGCCGGATTCACCCTTCTTC
CbPbp1_Fw	CTTTTGCTCACATGTCGACGCAATTGTTGGAATAATC
CbPbp1_Rv	ACTAACCATGTCGACAAATTTATAATGTCCTCTTGAACCC
CbEdc3_Fw	CTTTTGCTCACATGCTACTCTTCATTCTATAGCATG
CbEdc3_Rv	AGAAACCATGTCGACAGATTCGATAATTTCTAAAACTGT
ScHOG1_KD_Fw	AAAATCATGAAACCTTTTTCCACTGCA
ScHOG1_KD_Rv	TCTAATGGCAACTGGCTGAGATG

Journal of Cell Science • Supplementary information

ScHOG1_nP_Fw	GGCTTTGTTTCCACTAGATACTACAGG
ScHOG1_nP_Fw	AGCCATTTGAGGGTCTTGAATTCTTGCTAG
ScHOG1_CAAX_Fw	GGTTCTGGTGGTTGTTGTATTATTTCTTAACTGCAGGGAATTTAATC ATTTTCAAC
ScHOG1_CAAX_Rv	TTTATATAATTCATCCATACCTAAAGTAATACCAG
ScHOG1_350_Rv	ATCACTGCCACCAATCTTATGG
ScHOG1CTag_Fw	CGGTAACCAGGCCATACAGTACGCTAATGAGTTCCAACAGGTGAG CAAGGGCGAGGAGCT
ScHog1CTag_Rv	GAAGTAAGAATGAGTGGTTAGGGACATTAAAAAAACACGTCGACC TGTATCGCTCAAAAG
ScHog1_(351-435)_Fw	CAACAACAACAGCTGGGACAGATTGATATATCTGCC
ScHog1_(351-435)_Rv	TTAAATTCCCTGCAGTTATTTATATAATTCATCCATACCTAAAGTAA TAC
Zhog1_UPfw	CGTTTAATAAAGCCAGCCATTTAGATCGTCTAGACTAACCTATACG GGTTTAATGCC
Zhog1_UPrv	TGAAGCTATGGTGTGGAAGACTGCCGGTTTATCCTC
Zhog1_DWfw	TTTGGTCATGAGATCCTGTTCTGCCAAGGACAAGC
Zhog1_DWrv	GGCATTAAACCCGTATAGGTTAGTCTAGACGATCTAAATGGCTGGC TTTATTAAACG
pPICZ_Zeo_fw	CACACCATAGCTTCAAAATGTTTCTAC
pPICZ_Zeo_rv	GATCTCATGACCAAAATCCCTTAAC
PpHog1IF_fw	GGTACCCGGGGATCCCTAACCTATACGGGTTTAATGCC
PpHog1IF_rv	CAGCTCGAGACTAGTTTGATCCTCAACTTGATGGAAGTC

Journal of Cell Science • Supplementary information

Table S5. Plasmids used in this study.

Designation	Description	Reference
S. cerevisiae		
pMO152	EGFP *LEU2*	Oku *et al*. (In press)
C. boidinii		
SK+SPR	*URA3*	(Sakai & Tani 1992)
pHC100	Hog1-UPregion *URA3*	This study
pHC101	Hog1-UPregion Hog1-DOWNregion *URA3*	This study
pKK001	P_{CbACT1}Venus URA3	(Kawaguchi et al 2011)
pHC200	P_{CbHOG1}*CbHOG*1-Venus *URA3*	This study
pHC300	P_{CbACT1}*ScHOG1*-Venus URA3	This study
pHC201	P_{CbHOG1}*CbHOG1*Δ(1-10)-Venus *URA3*	This study
pHC202	P_{CbHOG1}*CbHOG1*Δ(1-17)-Venus *URA3*	This study
pHC203	P_{CbHOG1}*CbHOG1*Δ(1-20)-Venus *URA3*	This study
pHC204	P_{CbHOG1}*CbHOG1*Δ(1-30)-Venus *URA3*	This study
pHC205	P_{CbHOG1}*CbHOG1*Δ(1-41)-Venus *URA3*	This study
pHC206	P_{CbHOG1}*CbHOG1*Δ(348-398)-Venus *URA3*	This study
pHC207	P_{CbHOG1}*CbHOG1*Δ(318-398)-Venus *URA3*	This study
pHC208	P_{CbHOG1}*CbHOG1*Δ(300-398)-Venus *URA3*	This study
pHC209	P_{CbHOG1}*CbHOG1*(1-20)-Venus *URA3*	This study
pHC210	P_{CbHOG1}*CbHOG1*(1-30)-Venus *URA3*	This study
pHC211	P_{CbHOG1}*CbHOG1*(1-40)-Venus *URA3*	This study
pHC212	P_{CbHOG1}*CbHOG1*(1-50)-Venus *URA3*	This study
pHC213	P_{CbHOG1}*CbHOG1*(346-398)-Venus *URA3*	This study
pHC214	P_{CbHOG1}*CbHOG1*Δ(25-30)-Venus *URA3*	This study
pHC215	P_{CbHOG1}*CbHOG1*Δ(35-40)-Venus *URA3*	This study
pHC216	P_{CbHOG1}*CbHOG1*Δ(38-45)-Venus *URA3*	This study
pHC217	P_{CbHOG1}*CbHOG1*Δ(39-45)-Venus *URA3*	This study
pHC218	P_{CbHOG1}*CbHOG1*Δ(40-45)-Venus *URA3*	This study
pHC219	P_{CbHOG1}*CbHOG1*Δ(43-45)-Venus *URA3*	This study
pHC220	P_{CbHOG1}*CbHOG1* (K50R)-Venus *URA3*	This study
pHC221	P_{CbHOG1}*CbHOG1* (K50R)-mCherry *URA3*	This study
pSPM001	P_{CbACT1} mCherry *URA3*	(Shiraishi et al 2015)
pHC400	P_{CbHOG1}*CbHOG1*-mCherry *URA3*	This study
pHC401	P_{CbPAB1}*CbPAB1*-Venus *URA3*	This study
pHC402	P_{CbPAB1}*CbPAB1*-Venus *LEU2*	This study
pHC403	P_{CbPAB1}*CbPBP1*-mCherry *URA3*	This study
pHC404	P_{CbPAB1}*CbEDC3*-Venus *URA3*	This study
pHC405	P_{CbPAB1}*CbEDC3*-Venus *LEU2*	This study
pHC500	P_{CbACT1}*ScHOG1*-Venus *URA3*	This study
pHC501	P_{CbACT1}*ScHOG1*-K52R-Venus *URA3*	This study
pHC502	P_{CbACT1}*ScHOG1*-T174A/Y176F-Venus *URA3*	This study
pHC503	P_{CbACT1}*ScHOG1*-Venus-CAAX^{Ras2} *URA3*	This study
pHC504	P_{CbACT1}*ScHOG1*(1-350)-Venus *URA3*	This study
pHC505	P_{CbHOG1}*CbHOG1- ScHOG1*(351-435)-Venus *URA3*	This study
P. pastoris		
pPICZ A	*P. pastoris* expression vector, Zeo^r	Purchased from Invitrogen
pHP001	PpHog1-UPregion PpHog1-DOWNregion Zeocin	This study
nNT204	pIB1 *ARG4*	(Tamura et al 2010)
pHP100	P_{PpHOG1}*PpHOG1*-YFP *ARG4*	This study

References for Tables S3, S4, and S5

Brachmann, C. B., Davies, A., Cost, G. J., Caputo, E., Li, J., Hieter, P. and Boeke, J. D. (1998). Designer deletion strains derived from *Saccharomyces cerevisiae* S288C: a useful set of strains and plasmids for PCR-mediated gene disruption and other applications. *Yeast* **14**, 115-132.

Kawaguchi, K., Yurimoto, H., Oku, M. and Sakai, Y. (2011). Yeast methylotrophy and autophagy in a methanol-oscillating environment on growing *Arabidopsis thaliana* leaves. *PloS One* **6**, e25257.

Sakai, Y., Kazarimoto, T. and Tani, Y. (1991). Transformation system for an asporogenous methylotrophic yeast, *Candida boidinii*: cloning of the orotidine-5'-phosphate decarboxylase gene (*URA3*), isolation of uracil auxotrophic mutants, and use of the mutants for integrative transformation. *J. Bacteriol.* **173**, 7458-7463.

Sakai, Y., Koller, A., Rangell, L. K., Keller, G. A. and Subramani, S. (1998). Peroxisome degradation by microautophagy in *Pichia pastoris*: identification of specific steps and morphological intermediates. *J. Cell Biol.* **141**, 625-636.

Sakai, Y. and Tani, Y. (1992). Directed mutagenesis in an asporogenous methylotrophic yeast: cloning, sequencing, and one-step gene disruption of the 3-isopropylmalate dehydrogenase gene (*LEU2*) of *Candida boidinii* to derive doubly auxotrophic marker strains. *J Bacteriol.***174**, 5988-5993.

Shiraishi, K., Oku, M., Kawaguchi, K., Uchida, D., Yurimoto, H. and Sakai, Y. (2015). Yeast nitrogen utilization in the phyllosphere during plant lifespan under regulation of autophagy. *Sci. Rep.* **5**, 9719.

Tamura, N., Oku, M. and Sakai, Y. (2010). Atg8 regulates vacuolar membrane dynamics in a lipidation-independent manner in *Pichia pastoris*. *J. Cell Sci.* **123**, 4107-4116.

Tani, Y., Sakai, Y. and Yamada, H. (1985). Isolation and Characterization of a Mutant of a Methanol Yeast, *Candida boidinii* S2, with Higher Formaldehyde Productivity. *Agric. Biol. Chem.* **49**, 2699-2706.

Journal of Cell Science • Supplementary information

SUPPLEMENTARY FIGURES

Fig. S1

A

```
CbHog1          -MAQE-FTRTQIFGTIFETTNRYSDLNPVGMGAFGLVCAAKDKLTNQNVAIKKVMKPFST 58
ScHog1          MTTNEEFIRTQIFGTVFEITNRYNDLNPVGMGAFGLVCSATDTLTSQPVAIKKIMKPFST 60
PpHog1          -MSQEKFTRTQIFGTIFETTARYDELNPVGMGAFGLVCSAKDKLTEQQVAIKKIMKPFST 59
SpSty1          ---MAEFIRTQIFGTCFEITTRYSDLQPIGMGAFGLVCSAKDQLTGMNVAVKKIMKPFST 57
                      * ******* ** * **.:*:*:*********:*.* **   **:**:******

CbHog1          AVLAKRTYRELKLLNHLRHENLISLDDIFLSPLEDIYFVTELQGTDLHRLLTSRPLEKQF 118
ScHog1          AVLAKRTYRELKLLKHLRHENLICLQDIFLSPLEDIYFVTELQGTDLHRLLQTRPLEKQF 120
PpHog1          PVLAKRTYRELKLLNHLRHENLITLTDIFLSPLEDIYIVTELQGTDLHRLLTSRPLEKQF 119
SpSty1          PVLAKRTYRELKLLKHLRHENIISLSDIFISPFEDIYFVTELLGTDLHRLLTSRPLETQF 117
                .*************:******:* * ***:**:****:**** ******** :****.**

CbHog1          IQYFLYQILRGLKFVHSSGVIHRDLKPSNILINENCDLKICDFGLARVQDPQMTGYVSTR 178
ScHog1          VQYFLYQILRGLKYVHSAGVIHRDLKPSNILINENCDLKICDFGLARIQDPQMTGYVSTR 180
PpHog1          IQYFLYQILRALKYVHSAGVIHRDLKPSNILINENCDLKICDFGLARIQDHQMTGYVSTR 179
SpSty1          IQYFLYQILRGLKFVHSAGVIHRDLKPSNILINENCDLKICDFGLARIQDPQMTGYVSTR 177
                :*********.**:***:*****************************:** *********

CbHog1          YYRAPEIMLTWQKYDTEVDIWSAGCIFAEMIEGKPLFPGKDHVHQFSIITELLGSPPKDV 238
ScHog1          YYRAPEIMLTWQKYDVEVDIWSAGCIFAEMIEGKPLFPGKDHVHQFSIITDLLGSPPKDV 240
PpHog1          YYRAPEIMLTWQKYDTEVDIWSAGCIFAEMIEGKPLFPGKDHINQFSIITELLGSPPTDV 239
SpSty1          YYRAPEIMLTWQKYNVEVDIWSAGCIFAEMIEGKPLFPGRDHVNQFSIITELLGTPPMEV 237
                **************:.**********************:**::******:***:** :*

CbHog1          IDTICSENTLRFVQSLPHRDPIPFNEKFKGVEPEAIDLLSKMLVFDPRKRVTAEQALEHE 298
ScHog1          INTICSENTLKFVTSLPHRDPIPFSERFKTVEPDAVDLLEKMLVFDPKKRITAADALAHP 300
PpHog1          IDTICSENTLRFVQSLPHREPVPLIERFQGVEPVAIDLLEKMLVFDARKRITAEESLAHE 299
SpSty1          IETICSKNTLRFVQSLPQKEKVPFAEKFKNADPDAIDLLEKMLVFDPRKRISAADALAHN 297
                *:****:***:** ***::: :*: *:*: .:* *:***.******.:**::* ::* *

CbHog1          YLSPYHDPTDEPVAEEKFDWSFNDADLPVDTWRVMMYSEILDFHQVEGAEADALQQQVQG 358
ScHog1          YSAPYHDPTDEPVADAKFDWHFNDADLPVDTWRVMMYSEILDFHKIGGSDGQIDISATFD 360
PpHog1          YLEPYHDPTDEPVAAEKFDWSFNDADLPVDTWRVMMYSEILDFHQVEDQ----------- 348
SpSty1          YLAPYHDPTDEPVADEVFDWSFQDNDLPVETWKVMMYSEVLSFHNMDNELQS-------- 349
                *  ***********   *** *:* ****:**:******:*.**::

CbHog1          QYEHSMTLQQQQQQHQIQKQQELQENELLQQQQQQQQQQL-------------------- 398
ScHog1          DQVAAATAAAAQAQAQAQAQVQLNMAAHSHNGAGTTGNDHSDIAGGNKVSDHVAANDTIT 420
PpHog1          ------------------------------------------------------------
SpSty1          ------------------------------------------------------------

CbHog1          ---------------
ScHog1          DYGNQAIQYANEFQQ 435
PpHog1          ---------------
SpSty1          ---------------
```

B

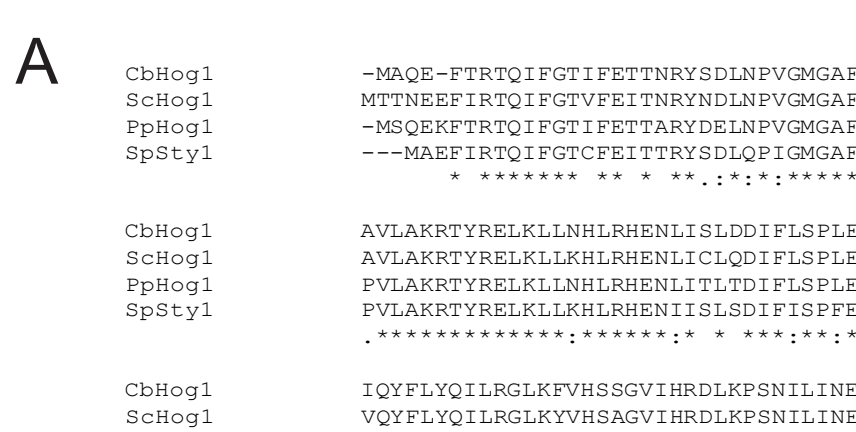

C

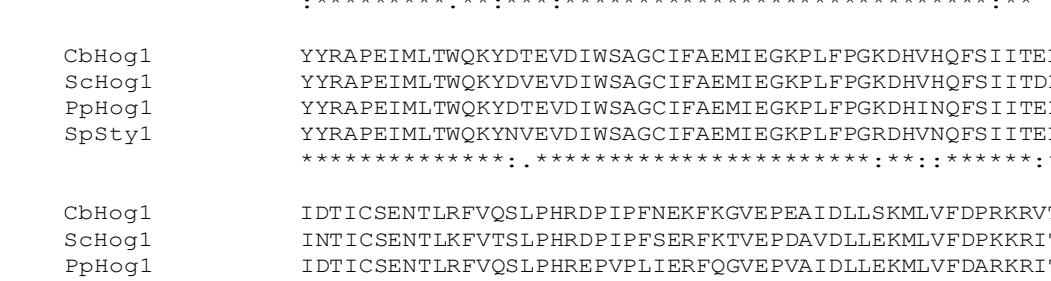

Journal of Cell Science • Supplementary information

Fig. S1. CbHog1 is required for tolerance to high salt stress. (A) Alignment of the amino acid sequences of Hog1 homolog proteins from four yeast species, *C. boidinii*, *S. cerevisiae*, *P pastoris,* and *S. pombe*. The CLUSTLW program was used to align the amino acid sequences of CbHog1, ScHog1, PpHog1 and SpSty1. The residues mutated in this study are marked in red. (B) Microscopic images of the *C. boidinii hog1*Δ strain expressing CbHog1-Venus. Cells were grown to early log phase in SD medium and shifted to SD medium supplemented with 0.5 M NaCl as high-osmolarity stress. DAPI was used for nuclear staining. Merged images were generated by combining the Venus (green) and DAPI (blue) fluorescence images. (C) Growth assay under high osmotic condition. The wild-type and the indicated mutant strains of *C. boidinii* were grown to early log phase, adjusted to OD_{610} = 1, and 3 μL of each ten-fold serial dilutions were dropped onto YPD plates with or without 0.5 M NaCl. Cells were incubated at 28˚C and cell growth was scored after 2 days.

Journal of Cell Science • Supplementary information

Fig. S2

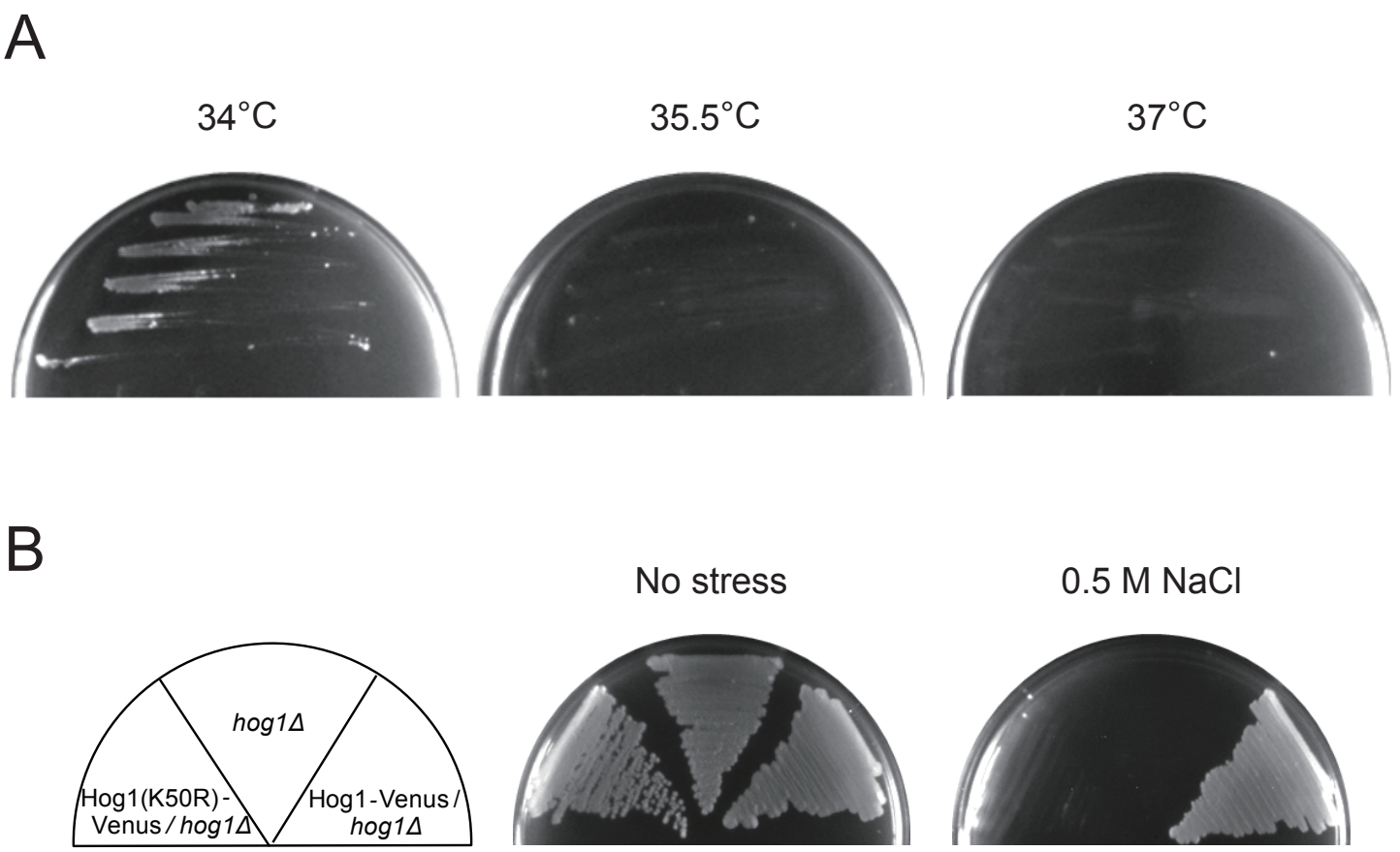

Fig. S2. Growth of *C. boidinii* strains under high-temperature or high-salt conditions. (A) Growth of *C. boidinii* under high-temperature conditions. Cells spread on the YPD plates were incubated at 34, 35.5 or 37˚C and cell growth was scored after 2 days. (B) Growth assay of the *Cbhog1Δ* strain and the *Cbhog1Δ* strains expressing CbHog1-Vunus or CbHog1(K50R)-Venus under high-salt condition. Cells were grown to early log phase, adjusted to OD_{610} = 1, and 3 µL of each ten-fold serial dilutions were dropped onto YPD plates without or with 0.5 M NaCl. Cells were incubated at 28˚C and cell growth was scored after 3 days.

Journal of Cell Science • Supplementary information

Fig. S3

A

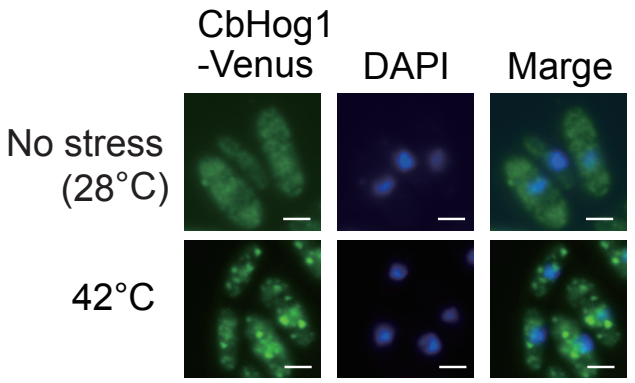

B

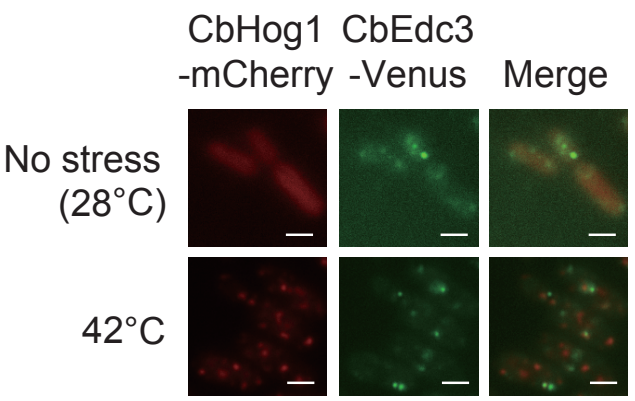

C

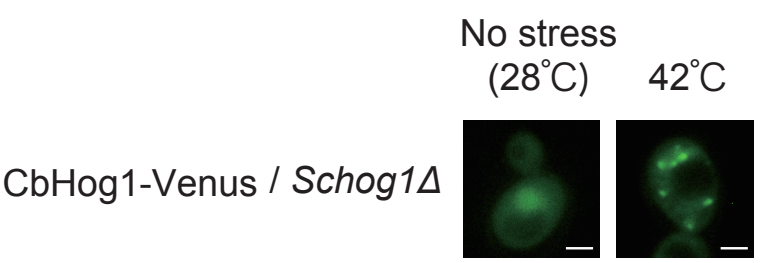

D

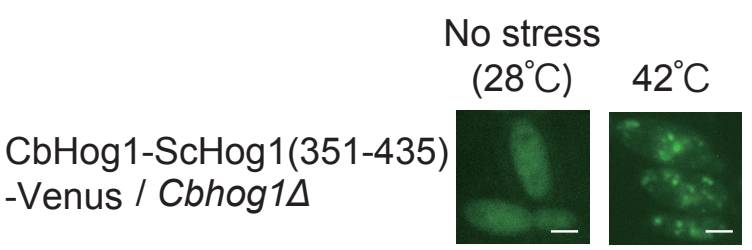

Journal of Cell Science • Supplementary information

Fig. S3. Microscopic images of various strains. (A) Microscopic images of the *C. boidinii* strain expressing CbHog1-Venus. Cells were grown to early log phase, and treated with indicated high-temperature stress for 30 min. Merged images were generated by combining the Venus (green) and DAPI (blue) fluorescence images. (B) Microscopic images of the *C. boidinii* strain expressing CbHog1-mCherry and CbEdc3-Venus. Cells were grown to early log phase, and treated with indicated high-temperature stress for 30 min. Merged images were generated by combining the mCherry (red) and Venus (green) fluorescence images. (C) Microscopic images of the *S. cerevisiae hog1*Δ strain expressing CbHog1-Venus under the control of the *ScHog1* promoter. Cells were grown to early log phase in SD medium, and treated with high-temperature stress (42˚C, 30 min). (D) Microscopic images of the *Cbhog1*Δ strain expressing CbHog1-ScHog1(351-435)-Venus. Cells were grown to early log phase in SD medium, and treated with high-temperature stress (42˚C, 30 min).

Journal of Cell Science • Supplementary information

Fig. S4

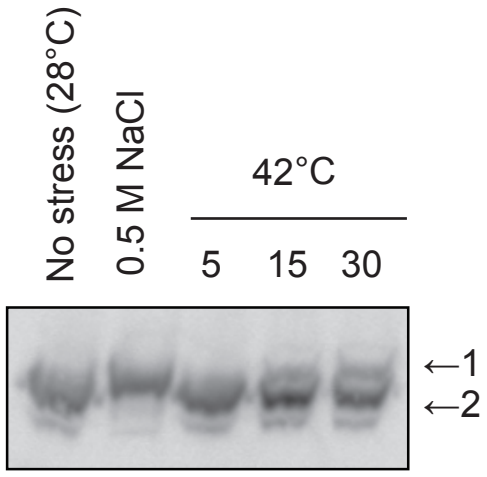

Fig. S4. CbHog1 is partially phosphorylated upon high-temperature stress. Immunoblot analysis of Venus-tagged Hog1 with Phos-tag SDS-PAGE under high-osmorality (0.5 M NaCl, 5 min) or high-temperature stress (42˚C, 5, 15 or 30 min). 1, phosphorylated CbHog1-Venus; 2, CbHog1-Venus.

Journal of Cell Science • Supplementary information